

## Organic Cage Compounds

# Synthesis of a Rigid $C_{3v}$ -Symmetric Tris-salicylaldehyde as a Precursor for a Highly Porous Molecular Cube

Sven M. Elbert, Frank Rominger, and Michael Mastalerz<sup>\*[a]</sup>

**Abstract:** The development of a synthetic approach to a  $C_{3v}$ -symmetric tris-salicylaldehyde based on triptycene is presented. The tris-salicylaldehyde is a versatile precursor for porous molecular materials, as demonstrated in the [4+4] condensation reaction with a triptycene triamine to form a molecular shape-persistent porous cube. The amorphous material of the molecular porous cube shows a very high

surface area of  $1014 \text{ m}^2 \text{ g}^{-1}$  (BET model) and a high uptake of  $\text{CO}_2$  (18.2 wt% at 273 K and 1 bar). Furthermore, during the multistep synthesis of the tris-salicylaldehyde precursor, a relatively rare (twofold) addition of the alkyne to the anthracene in the 1,4- and 1,4,5,8-positions have been found during a Diels–Alder reaction, as proven by X-ray structure analysis.

## Introduction

Donald Cram finished his Nobel lecture in 1987 with the fascinating topic of carcerands, which he conceptually called synthetic molecular cells,<sup>[1]</sup> and envisioned the manifold possibilities of such porous molecular structures. Nowadays, these kinds of molecular organic structures he termed carcerands are better known as organic cage compounds.<sup>[2]</sup> Indeed, since the first description of shape-persistent organic cage compounds by Vögtle and Kiggen, who synthesised them for the selective recognition of  $\text{Fe}^{3+}$ ,<sup>[3]</sup> interest in those structures gained a renaissance through the introduction of the concept of dynamic covalent chemistry (DCC).<sup>[4]</sup> By applying DCC, cage compounds are accessible in high yields from simple molecular building blocks.<sup>[5]</sup> It was again the group of Cram who applied this method in 1991 to connect two pre-organised molecular resorcinarene tetraldehydes with four phenylene diamines to form covalent organic capsules in a one-pot, eightfold imine condensation reaction in high yields.<sup>[6]</sup> Since then, the method has often been adopted to obtain organic cages in various geometries and sizes.<sup>[5, 7]</sup>

In 2009, Cooper et al.<sup>[8]</sup> and Atwood et al.<sup>[9]</sup> showed that organic cage compounds could be used as molecular units to create porous materials with a reported maximum measured surface area of  $624 \text{ m}^2 \text{ g}^{-1}$  (BET model). This approach to create porous materials simply by self-assembling molecules through weak interactions without making new bonds was unique at that time; the contribution from the groups of Cooper and Atwood could be seen as the birth of a new area in the field

of porous materials.<sup>[10, 11]</sup> Since then, we and others have shown that shape-persistent organic cage compounds can be used as molecular units to form porous materials with different pore sizes.<sup>[12, 13]</sup> Recently, we introduced the synthesis of a discrete boronic ester cage with pores in the mesoporous regime, exceeding 2 nm and very high surface areas of  $3758 \text{ m}^2 \text{ g}^{-1}$  (BET).<sup>[12f]</sup> With these values, this material based on discrete molecules is one of the most porous crystalline materials known and comparable to some of the best performing metal–organic frameworks (MOFs).<sup>[14]</sup> What distinguishes porous cages from other porous (three-dimensional network) materials is their solubility, and this has been exploited to process cage compounds for several purposes, for example, by embedding the cages into mesoporous silica or membranes to enhance gas sorption selectivity,<sup>[15, 16]</sup> making porous organic alloys;<sup>[17]</sup> bringing them onto the surface of quartz crystal microbalances to enhance the selective recognition of certain analytes in the vapour phase,<sup>[18]</sup> or post-functionalising them to change their chemical stability<sup>[18b, 19]</sup> or gas sorption properties.<sup>[20]</sup>

As mentioned above, several geometries have been realised for organic cages by applying DCC.<sup>[7, 21b]</sup> Although molecular cubes have been made previously by imine condensation, as well as boronic ester formation, they either have not been investigated in terms of porosity or collapse upon desolvation of the “virtually” porous material, due to the intrinsic flexibility of the molecular structures.<sup>[21]</sup>

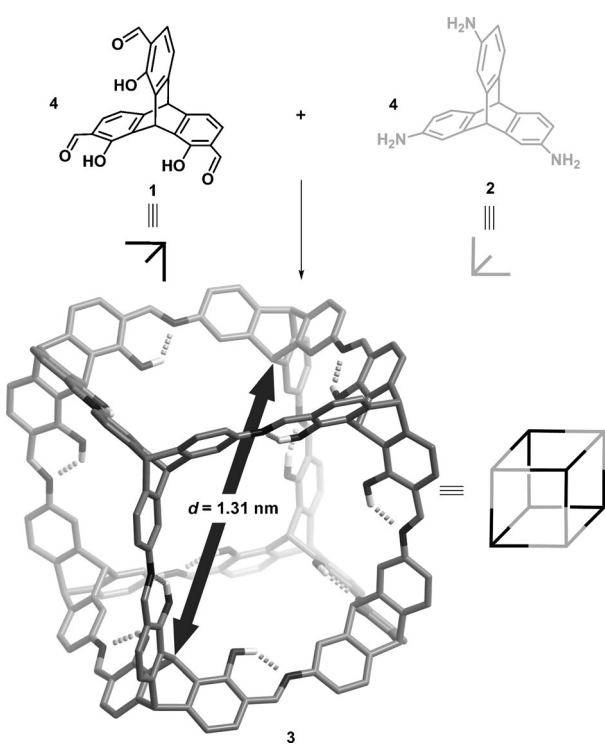
We envisioned that rigid  $C_{3v}$ -symmetric triptycene tris-aldehyde **1** could be a potential precursor for synthesising a cube in the stoichiometric [4+4] condensation reaction with triamine **2**<sup>[22]</sup> (Scheme 1), and due to its geometry and inherent rigidity should be stable enough to form a porous molecular material when evacuated.<sup>[11]</sup> Furthermore, the molecular structure of **3** contains relatively large quadratic windows (diameter = 1.01–1.14 nm) and a molecular void with a diameter of  $d = 1.31 \text{ nm}$  between two opposite triptycene bridgehead pro-

[a] S. M. Elbert, Dr. F. Rominger, Prof. Dr. M. Mastalerz

Organisch-Chemisches Institut  
Ruprecht-Karls-Universität Heidelberg  
Im Neuenheimer Feld 270, 69120 Heidelberg (Germany)  
E-mail: michael.mastalerz@oci.uni-heidelberg.de

 Supporting information for this article is available on the WWW under  
<http://dx.doi.org/10.1002/chem.201404829>.

tons. Molecule **3**, with the geometrical shape of an open cube without peripheral side chains, should not be able to pack tightly according to the concept of frustrated molecular packing.<sup>[23]</sup> Therefore, we assumed that cube **3**, and thus, tris-salicylaldehyde **1** would be an attractive synthetic target. Herein, we present the development of a synthetic method to the rigid precursor **1**. Through condensation reactions with **3**, a highly porous molecular cube is formed in the solid state with a high specific surface area of  $1014 \text{ m}^2 \text{ g}^{-1}$  and a narrow pore size distribution, absorbing up to 18.4 wt% of  $\text{CO}_2$  at 273 K and 1 bar.



**Scheme 1.** Synthesis of a rigid [4+4] cube (**3**) in a twelvefold Schiff base condensation reaction of four molecules of **1** and four molecules of **2**. The arrow shows the pore diameter of about 1.31 nm, as extracted from an AM1-optimised model.

## Results and Discussion

### Synthesis and characterisation of the triptycene tris-salicylaldehyde precursor

Non-substituted triptycene<sup>[24]</sup> is known to preferably react in electrophilic aromatic substitution reactions at the 2,6,14- and 2,7,14-positions<sup>[22, 25, 26]</sup> (for numbering of the positions on the triptycene scaffold, see Figure 1) due to the so-called fused *ortho* effect.<sup>[27]</sup> Therefore, functional groups in the 1-, 8-, 13- or 16-positions have to be introduced into the triptycene scaffold during the Diels–Alder reaction by choosing the corresponding substituted aryne and anthracene as starting materials. For instance, in 1971, Mori et al.<sup>[28]</sup> presented the first examples of such substituted triptycenes by using 1,8-dichloroanthracene and 6-chloroanthranilic acid as reactants to obtain the so-called *syn* (1,8,13-substituted) and *anti* (1,8,16-substituted) tri-

chlorotriptycenes in a *syn/anti* ratio of 1.0:1.9. They attributed this non-statistical ratio to the inductive effect of the chloro substituents.<sup>[28]</sup> In 1986, Rogers and Averill used the idea from Mori et al. and extended the functionalities from chloro to cyano, acetic acid methyl ester and methyl substituents, and also synthesised trisubstituted triptycenes with mixed functional groups.<sup>[29]</sup>

To synthetically achieve tris-salicylaldehyde **1**, the tris-hydroxy-substituted scaffold has to be formed within such a Diels–Alder reaction in a fluoride-mediated addition of triflate **4**<sup>[30]</sup> to 1,8-dimethoxyanthracene (**5**).<sup>[31]</sup> Addition of the in situ formed aryne to positions 9 and 10 of the anthracene should lead to the triptycenes **6a** and **6b** (Scheme 2).

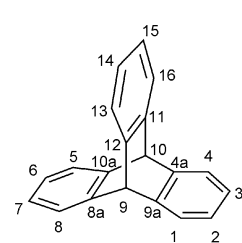
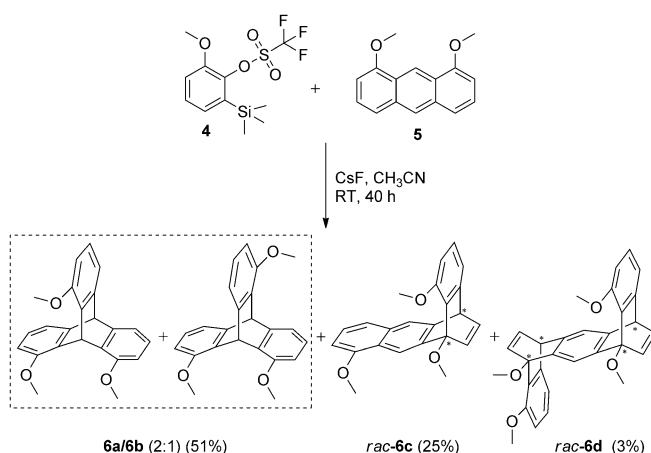


**Figure 1.** Numbering of triptycene consistent with the 9,10-dihydro-9,10-o-benzenoanthracene nomenclature.



**Scheme 2.** Diels–Alder reaction of triflate **4** and anthracene **5** to the desired trisubstituted triptycenes **6a/6b** and the unexpected by-products **rac-6c** and **rac-6d**. The dashed box marks an inseparable mixture.

After reacting triflate **4** and anthracene **5** in dry acetonitrile with caesium fluoride as a base for 40 h, monitoring of the reaction by TLC showed four products and the  $^1\text{H}$  NMR spectrum of the crude product revealed some characteristic signals in the region around  $\delta = 5$  ppm, which could not be assigned to triptycene bridgehead protons (Figure 2a).

Due to their low solubility, triptycenes **6a** and **6b** could be isolated in 51% yield as a white solid after washing the crude product with water, methanol and  $\text{CH}_2\text{Cl}_2$ . By  $^1\text{H}$  NMR spectroscopic analysis of the remaining white solid, it was confirmed that a 2:1 mixture of *syn*-**6a** and *anti*-**6b** has been formed (Figure 2b). The ratio of the triptycene isomers was estimated by integration of the signals resonating at  $\delta = 5.53$  and 5.85 ppm, which could be assigned to bridgehead protons  $\text{H}^\text{e}$  and  $\text{H}^{\prime\prime\prime}$  of the  $C_{3v}$ - and  $C_s$ -symmetric triptycenes **6a** and **6b**, respectively. The ratio of 2:1 deviates from the statistically expected 1:1 ratio and is comparable to the first findings by Mori et al.<sup>[28]</sup>

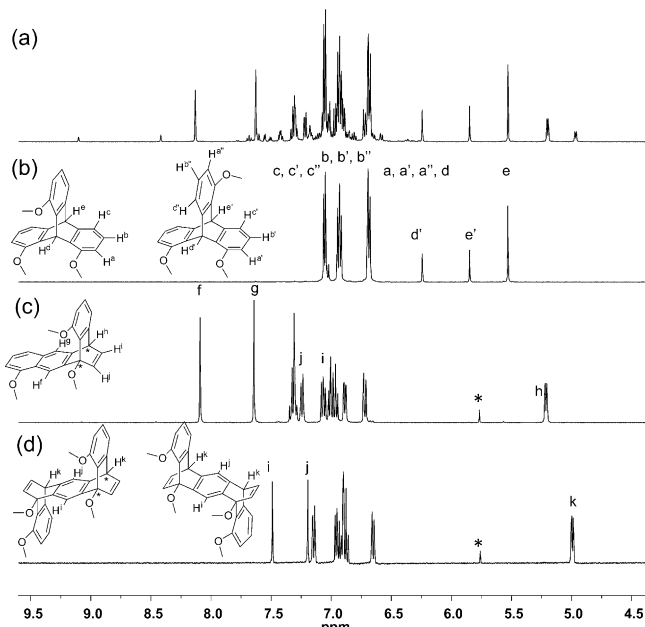


**Figure 2.**  $^1\text{H}$  NMR spectra of: a) the crude product of the Diels–Alder reaction depicted in Scheme 2, b) mixture of **6a**/**6b** isolated in a 2:1 ratio, c) *rac*-**6c**, and d) *rac*-**6d**. All spectra were recorded in  $[\text{D}_6]\text{DMSO}$  at 500 (a and b) and 400 MHz (c and d). Spectra in a) and b) were measured at 375 K. The asterisks indicate residual  $\text{CH}_2\text{Cl}_2$ .

This non-statistical product distribution was already observed by others<sup>[28,29,32]</sup> and could be explained by frontier orbital controlled regioselectivity during cycloaddition, similar to the descriptions of Rogers and Averill.<sup>[29]</sup> In the [4+2] cycloaddition, the anthracene represents the diene component. If the  $\pi$  electrons of the central ring are involved in the reaction, the mesomeric effects of the methoxy substituents have to be taken into account, which means that a positive partial charge is generated at position 9, and there is a negative partial charge at position 10 (Figure 3, left). The aryne acts as a dienophile in the reaction. The formally triple-bond electrons involved are located in  $\text{sp}^2$  orbitals that lie in the  $\sigma$ -bond plane of the molecular scaffold.<sup>[33]</sup> Therefore, here the inductive effect of the methoxy group over the  $\sigma$ -bond scaffold has to be taken into account, rather than the mesomeric effect; this results in a negative partial charge at position 2 and a positive partial charge at position 3 of the aryne (Figure 3, right).

In principle, position 9 of the anthracene preferably interacts with position 2 of the aryne by attractive coulomb interactions, which is a rational explanation for the difference in the observed 2:1 *syn/anti* ratio from a statistical 1:1 mixture, similar to that described previously by Mori et al.<sup>[28]</sup>

The extract in  $\text{CH}_2\text{Cl}_2$  contained two more Diels–Alder products, which could be isolated by column chromatography. The molecular mass of the first by-product, **6c**, was  $m/z$  344 (El-MS), which was the same as that for triptycenes **6a** and **6b**. By  $^1\text{H}$  NMR spectroscopy, it was found that **6c** was the 1,4-adduct of the Diels–Alder reaction (Scheme 2). Two characteristic singlets at  $\delta=8.09$  and 7.64 ppm can be assigned to protons  $\text{H}^{\text{f}}$  and  $\text{H}^{\text{g}}$  of the naphthyl substructure (Figure 2c). At  $\delta=5.22$  ppm, the bridgehead proton  $\text{H}^{\text{h}}$  resonates as a doublet of

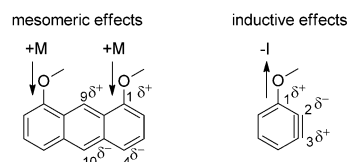


**Figure 3.** Left: mesomeric effects of the methoxy groups on 1,8-dimethoxyanthracene (**5**). Right: inductive effects of the methoxy group on a methoxy-substituted aryne.

doublets ( $J=6.1$  and 1.4 Hz) with coupling to the olefinic protons  $\text{H}^{\text{i}}$  ( $\delta=7.07$  ppm,  $J=6.0$  Hz) and  $\text{H}^{\text{j}}$  ( $\delta=7.24$  ppm,  $J=1.1$ –1.4 Hz). It was difficult to determine by 2D NMR spectroscopy methods whether the formation of the 1,4-adduct occurred in a *syn* or *anti* fashion. Therefore, we grew single crystals of **6c** suitable for X-ray analyses<sup>[34]</sup> by slow diffusion of *n*-pentane into a solution of **6c** in  $\text{CH}_2\text{Cl}_2$  (Figure 4a). X-ray analyses proved the *syn* addition of the aryne to the 1,4-position of the anthracene to give *rac*-**6c** (for detailed information on the crystal structure, see Table S1 in the Supporting Information).

Such 1,4-adducts were first reported by Klanderman<sup>[35]</sup> and recently by McKeown and co-workers,<sup>[36]</sup> but are still a rare exception in the reaction of arynes and anthracenes.<sup>[37]</sup> Again, this rare cycloaddition can only be explained by frontier orbital controlled regioselectivity, similar to the situation explained above. The second isolated fraction showed a less complicated signal pattern in the  $^1\text{H}$  NMR spectrum than that of **6c** (Fig-

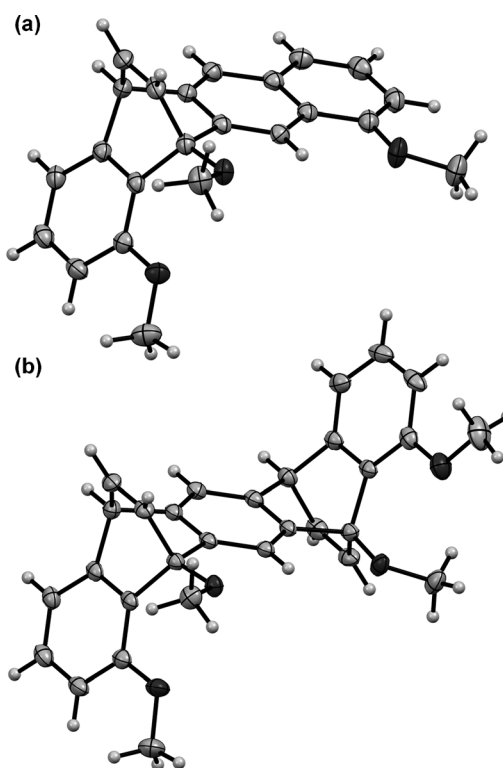


**Figure 4.** Single-crystal X-ray structures of: a) *rac*-**6c**, and b) *rac*-**6d**. Only one isomer of each is depicted. Carbon: light grey, oxygen: dark grey, hydrogen: white. Thermal ellipsoids are shown with 50% probability. For further details, see Tables S1 and S2 in the Supporting Information.

ure 2c) and in the EI-MS a mass signal of  $m/z$  450 was found, which corresponded to the twofold addition of the aryne to the anthracene.  $^1\text{H}$  NMR spectroscopy indicates the structure of **6d** because of the characteristic singlets that can be assigned to protons  $\text{H}^i$  ( $\delta=7.49$  ppm) and  $\text{H}^j$  ( $\delta=7.19$  ppm) of the central aromatic ring.

Those singlets appear to be shifted to high field relative to those of **6c**. Even more characteristic is the signal of bridgehead proton  $\text{H}^k$  at  $\delta=4.99$  ppm. Through crystallisation, again from  $\text{CH}_2\text{Cl}_2$  and *n*-pentane, suitable crystals of *rac*-**6d** have been obtained (for detailed information, see Table S2 in the Supporting Information), which further proved the twofold *syn* addition in the formation of the 1,4,5,8-bis adducts as a racemic mixture. Although **6d** has been isolated in only 3% yield, it should be noted that 1,4,5,8-bisadducts have not been described in the cycloaddition of arynes to anthracenes and, to the best of our knowledge, a similar product has only been observed in the twofold addition of dicyanoacetylene to anthracenes with bulky phenyl substituents at positions 9 and 10.<sup>[38]</sup> In this context, it is worth mentioning that, for the formation of *rac*-**6d**, in principle, a [4+2] Diels–Alder reaction at the naphthalene scaffold of *rac*-**6c** has to occur; which is generally rarely observed.<sup>[39]</sup> Most interestingly, other regiosomeric by-products of the 1,4-additon and the 1,4,5,8-twofold addition have not been found,<sup>[40]</sup> which once more could be explained by the directing effects of the methoxy substituents in the reaction, as discussed above.

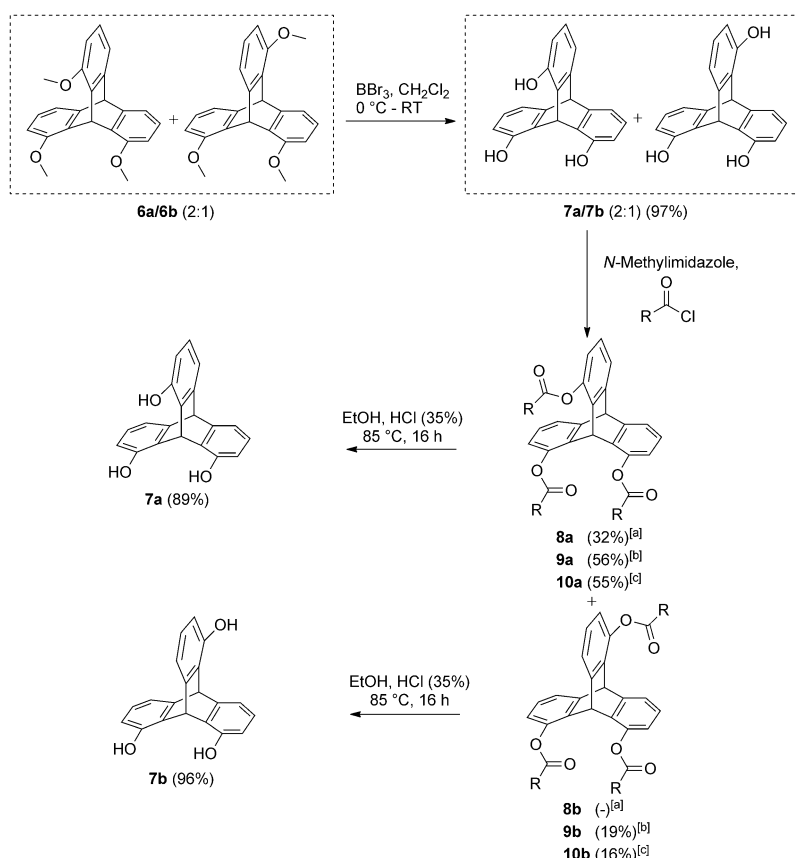
To continue with the synthetic sequence to form tris-salicylaldehyde **1**, the two regioisomers **6a** and **6b** have to be separated prior to further reactions at the aromatic scaffold. Although for a dilute sample of the mixture of triptycene **6a/b** two fractions were detectable by analytical HPLC, this method could not be used for larger quantities, simply because of the very low solubilities of triptycenes **6a** and **6b**. Interestingly, this is in accordance with other triptycene derivatives with three substituents in positions 1, 8, 13 or 16 and seems to be less dependent on the nature of the substituent itself.<sup>[28, 29, 32]</sup>

To separate the two isomers **6a** and **6b**, they had to be transformed into soluble derivatives to make them processable, for example, by column chromatography. Therefore, the methyl ethers were first quantitatively cleaved by  $\text{BBr}_3$  to give the corresponding triptycenes **7a/b** (Scheme 3). The hydroxyl com-

pounds **7a** and **7b** are not significantly more soluble than **6a** and **6b**; therefore, these compounds are also not possible to separate by column chromatography on reasonable scales. Several attempts to fractionally crystallise the mixtures were not successful. To obtain soluble derivatives of **7a/b**, esterification with capronyl chloride in the presence of methyl imidazole to the corresponding esters **8a/b** was performed (Scheme 3).

To our delight, the desired  $C_{3v}$ -symmetric ester **8a** crystallised from the reaction mixture to give the pure compound in 32% yield. The structure was proven by  $^1\text{H}$  NMR spectroscopy by the appearance of just one set of signals for the aromatic protons ( $\delta=7.25$ , 7.00 and 6.79 ppm) and two distinct singlets for the bridgehead protons at  $\delta=5.82$  and 5.50 ppm. Furthermore, crystals suitable for X-ray crystal-structure analysis were obtained (Figure 5 and Table S3 in the Supporting Information) and additionally proved the  $C_{3v}$ -symmetric structure of **8a**.

The mother liquor of crystallisation contained both isomers (*syn* and *anti*) in a ratio of approximately 1:1, as determined by the integration of characteristic signals in the  $^1\text{H}$  NMR spectrum. However, this mixture was difficult to separate by column chromatography, as originally intended. Nevertheless, this promising result of selective fractional crystallisation brought us to test other esterifications to separate the two isomers. Both the formed acetyl esters and benzyl esters showed



**Scheme 3.** Synthetic separation of *syn*- and *anti*-trisubstituted triptycenes. The dashed boxes mark inseparable mixtures. [a]  $\text{R}=\text{C}_5\text{H}_{11}$ , RT, 16 h; [b]  $\text{R}=\text{CH}_3$ ,  $\text{CH}_2\text{Cl}_2$ , 0°C–RT, 16 h; [c]  $\text{R}=\text{Ph}$ , RT, 16 h. Note: **7a** and **7b** were synthesized from **8a** and **8b** exclusively.

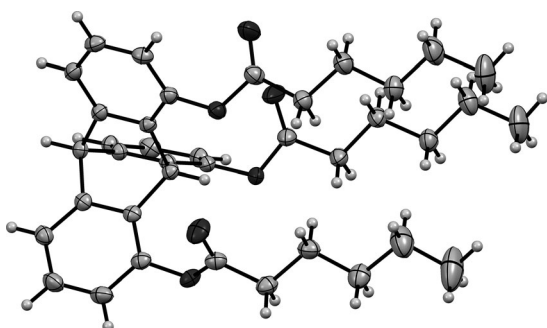


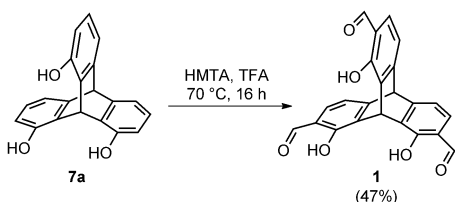
**Figure 5.** Single-crystal X-ray structure of triptycene tricapronyl ester **8a**. Only one molecule of the asymmetric unit is depicted. Carbon: light grey, oxygen: dark grey, hydrogen: white. Thermal ellipsoids are shown with 50% probability.

the same fractional crystallisation behaviour as the capronyl esters, giving the acetyl ester of **9a** in 43% yield and benzyl ester **10a** in 42% yield as fractionated crystals. In contrast to the capronyl esters, here, both isomers remaining in the mother liquor could be separated by column chromatography to give an additional 13% yield of *syn* isomers **9a** and **10a**, in addition to 19% of **9b** and 16% of **10b**. All isolated esters have been characterised by NMR spectroscopy, MS and IR spectroscopy; additionally, the purity was proven by elemental analysis (see the Experimental Section and the Supporting Information). For **9a**, **9b** and **10a**, crystals of suitable quality for X-ray structure analysis have also been obtained (see Tables S4–S6 in the Supporting Information).

The desired pure trihydroxytriptycene isomer **7a** was obtained in nearly quantitative yield by ester cleavage of **9a** in a mixture of ethanol and hydrochloric acid (Scheme 3). Under similar conditions, *anti*-trihydroxytriptycene **7b** was obtained in 96% yield from **9b**.

Finally, through the reaction of **7a** under Duff conditions,<sup>[41]</sup> tris-salicylaldehyde **1** was obtained in 47% yield as the sole regiosomer (Scheme 4).

The <sup>1</sup>H NMR spectrum of **1** shows a sharp signal at  $\delta=9.96$  ppm for the three aldehyde protons and a broad signal at  $\delta=11.00$  ppm, which corresponds to the hydroxyl protons. The signals of the bridgehead protons can be found at  $\delta=6.84$  ppm and at  $\delta=6.02$  ppm. CI-MS shows the signal of the molecular ion  $[M]^+$  at  $m/z$  386, as well as the signal of  $[M+H]^+$  with  $m/z$  387, which indicates the formation of **1**. By IR spectroscopy, the appearance of defined bands at  $\nu=1660$  (KBr pellet) or  $1649\text{ cm}^{-1}$  (Ge attenuated total reflectance (ATR)



**Scheme 4.** Selective formylation of **7a** in the *ortho* position to give tris-salicylaldehyde **1**. HMTA = hexamethylenetetramine, TFA = trifluoroacetic acid.

crystal, see the Supporting Information) clearly proved the introduction of formyl moieties and could be attributed to vibration of the carbonyl groups.

The selective formylation in the *ortho* position to the hydroxyl group of **7a** can be proven by 2D NMR spectroscopy (see the Supporting Information) and also by single-crystal X-ray analysis: crystals with sufficient quality have been obtained by slow diffusion of water into a solution of **1** in  $[\text{D}_6]\text{DMSO}$  inside an NMR tube (for data, see Table S7 in the Supporting Information).

The obtained crystal structure proves *ortho*-selective formylation as well as the proposed unidirectional orientation of all three salicylaldehyde functions (Figure 6a). The three aldehyde functions are co-planar to the aromatic phenyl rings. The average bond length of the C=O bonds is  $1.23\text{ \AA}$  slightly elongated in comparison to non-substituted benzaldehyde ( $1.21\text{ \AA}$ )<sup>[42]</sup> and the average phenolic C—O bond is in comparison to those in simple phenols, such as 4-*tert*-butyl phenol<sup>[43]</sup> shortened from  $1.39$  to  $1.36\text{ \AA}$ ; these both indicate hydrogen-bond-assisted resonance effects.<sup>[44]</sup> The molecules self-assemble anisotropically within the crystal through  $\pi$ — $\pi$  stacking (the distance between two adjacent aromatic rings is  $d=3.68\text{ \AA}$ ; see the green dotted line in Figure 6b) and form one-dimensional channels along the crystallographic *c* axis (Figure 6c) with a pore diameter of about  $0.7\text{ nm}$ . According to calculations by CrystalExplorer,<sup>[45]</sup> for **1** a specific surface area of  $374\text{ m}^2\text{ g}^{-1}$  should be accessible. However, investigations of the porosity of this material are beyond the scope of this contribution and investigations in this respect will be reported elsewhere.

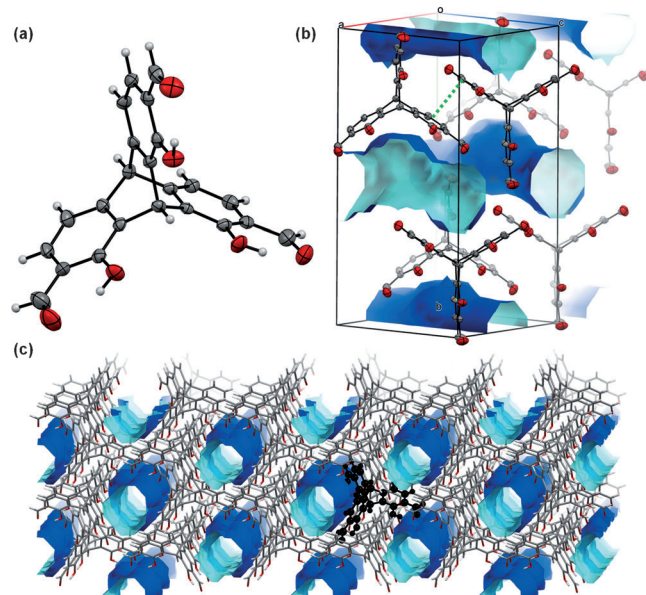


**Figure 6.** a) X-ray crystal structure of **1**. Thermal ellipsoids are shown with 50% probability. b) Enlarged packing of **1** within the unit cell. The green dotted line shows the  $\pi$ — $\pi$  stacking with a distance of  $d=3.68\text{ \AA}$ . Voids in the crystal are shown in blue and turquoise. c) Packing of **1** as a capped stick model and one-dimensional pores (blue and turquoise) formed along the crystallographic *c* axis. One molecule of **1** is shown in black as a ball and stick model. Carbon: grey; oxygen: red; hydrogen: white.

## Synthesis and characterisation of a porous [4+4] cube

Triptycene tris-salicylaldehyde **1** is a potential building block for condensation reactions. Before using **1** in the reaction with triamine **2** to synthesise a molecular cube, salicylimine **12** was synthesised in a threefold condensation with *para*-toluidine (**11**) in 73% yield (Scheme 5) as a model compound for spectroscopic comparison with molecular cube **3**.

The  $^1\text{H}$  NMR spectrum of **12** shows a characteristic singlet at  $\delta=8.93$  ppm for the three imine protons and the signal for the aldehydic protons at  $\delta=9.96$  ppm of the precursor tris-salicylaldehyde **1** are no longer detectable. The  $^{13}\text{C}$  NMR spectrum of **12** also reveals successful imine condensation through a signal at  $\delta=162.7$  ppm for the imine  $^{13}\text{C}$  nuclei; the signal for the aldehyde  $^{13}\text{C}$  nuclei of **1** at  $\delta=196.2$  ppm is no longer detectable. Suitable crystals of **12** for single-crystal X-ray analysis were obtained by vapour diffusion of *n*-pentane into a solution of **12** in  $\text{CH}_2\text{Cl}_2$  (Figure 7 and Table S8 in the Supporting Information). It is known that salicylimines can undergo reversible proton transfer to form their keto-enamine tautomer.<sup>[46]</sup> Tris-salicylimine **12** has an average bond length of  $d=1.35$  Å for the phenolic C–O bonds, which is comparable to those of tris-salicylaldehyde **1** and again shorter than that for simple phenols (1.39 Å);<sup>[43]</sup> thus, the imine–ol tautomer is more pronounced than the keto–amine tautomer. Furthermore, the length of the imine C=N bond ( $d=1.28$  Å) is slightly longer than that for non-hydrogen-bonded aromatic imines (1.25 Å).<sup>[47]</sup> These bond lengths are in a typical range for the proposed salicylimine structure at 200 K and again indicates hydrogen-bond-assisted resonance.<sup>[44]</sup> The absence of characteristic signals for the carbonyl groups in  $^{13}\text{C}$  NMR and IR spectroscopy indicate that **12** is also more likely to be present in the salicylimine tautomeric form at room temperature than in the ketoamine tautomer.

Cubic cage compound **3** was obtained in 65% yield by a twelvefold Schiff base reaction of tris-salicylaldehyde **1** and triaminotriptycene **2** after stirring the reaction mixture for 3 days at 120 °C in dry DMF (Schemes 1 and 5).<sup>[12b]</sup> It was found by MALDI-MS that the bright-yellow, still-wet solid showed a pronounced signal with a monoisotopic mass of  $m/z$

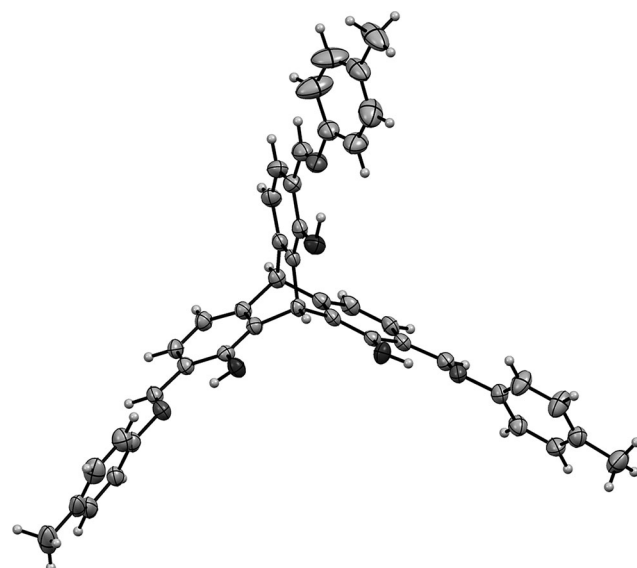


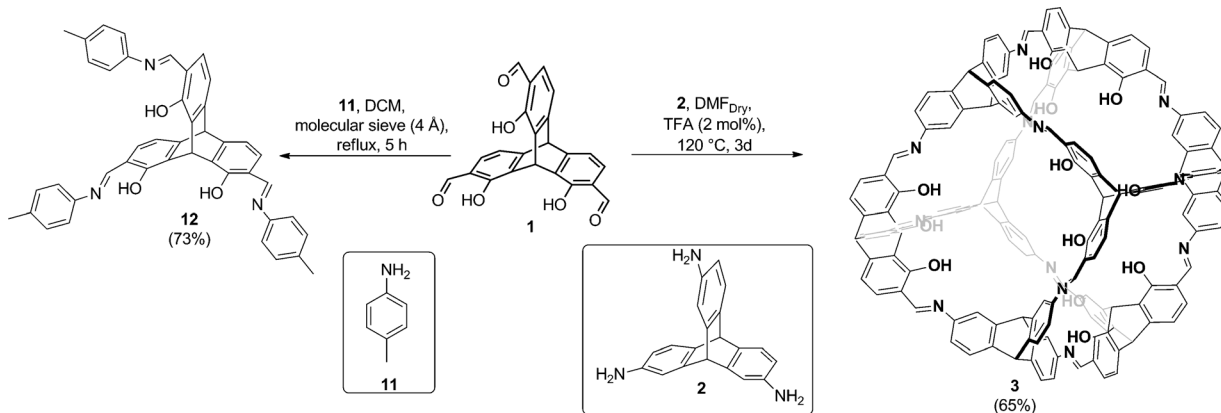
**Figure 7.** X-ray crystal structure of **12**. Carbon: light grey; oxygen: black; nitrogen: dark grey; hydrogen: white. Solvent molecules are omitted for clarity. Thermal ellipsoids are shown with 50% probability.

2524.78, which correlated with the calculated monoisotopic mass expected for cubic cage compound **3** ( $m/z$  2524.75). It is important to exchange DMF used as a medium in the reaction by immersing the material in dry diethyl ether (3 × 24 h) to allow cage compound **3** to remain stable towards filtration. Water has to be strictly excluded.<sup>[48]</sup>

When carefully worked up, dried cage compound **3** showed only one sharp signal with the expected isotopic pattern ( $m/z$  2525.3) by MALDI-TOF (Figure 8) and HRMS (MALDI;  $m/z$  2524.78; see the Supporting Information).

Similar to the [4+6] *exo*-functionalised cage we described earlier,<sup>[12b]</sup> lower reaction temperatures mainly result in the formation of intermediates, as determined by MALDI-TOF MS.

To exclude the formation of catenanes, a mass spectrum in the range of  $m/z$  750–8000 was recorded and no further signals were detected (see also the Supporting Information).<sup>[12g,49]</sup> Additionally, no smaller (e.g., [1+2] or [2+1]) or larger (up to



**Scheme 5.** Condensation reactions of tris-salicylaldehyde **1** with **11**, to give model compound **12**, and with triaminotriptycene **2** to give [4+4] cage compound **3**.

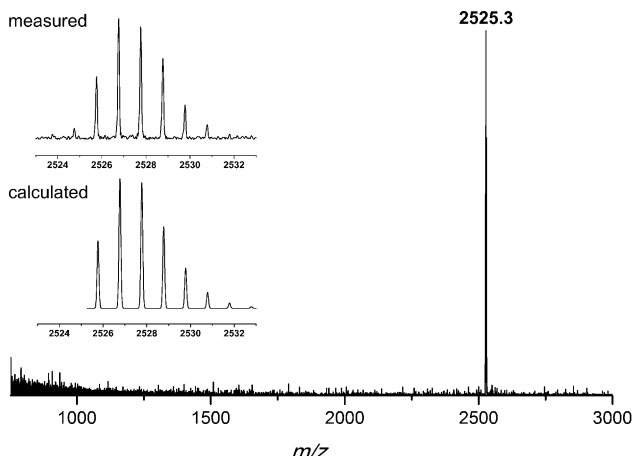


**Figure 8.** MALDI-TOF MS of cage **3**. The insets show the isotopic pattern measured by HRMS (MALDI; top) and the calculated isotopic pattern (bottom).

[12+13] or [13+12]) condensation products of the reaction of tris-aldehyde **1** and triamine **2** could be detected either, if it is assumed that these products or intermediates were similarly ionised through the methods typically applied in MALDI. Unfortunately, cage compound **3** is not soluble enough for characterisation by NMR spectroscopy methods (see also discussion below) in solution. For insoluble molecular cages, it has been controversially discussed, whether the compound contains kinetically formed polymers in different ratios as insoluble by-products or not. Thermodynamically, almost complete conversion of the precursors to cages **3** should be entropically favoured, in comparison to a polymeric mixture. If no polymer is formed kinetically, it seems to be reasonable to assume that the thermodynamic equilibrium is reached with the formation of cage compound **3**. Therefore, we monitored the condensation reaction by MALDI MS (see the Supporting Information). It can clearly be seen that, at the beginning of the reaction, smaller soluble intermediates, such as [1+1] and [1+2] condensation products, are formed and are consumed with increasing reaction time to form larger (still soluble) molecular intermediates, such as [2+2] and [2+3] condensation products. When the first precipitation occurs, the [4+4] cage compound **3** is detected. Further monitoring revealed that, with increasing reaction time, smaller intermediates were consumed and finally exclusively cage compound **3** could be detected. Based on these observations and thermodynamic assumptions, it can be concluded that no or very little polymeric by-products are formed.

To further characterise cage compound **3**, a  $^{13}\text{C}$  CP MAS solid-state NMR spectrum was recorded and the signals were compared with a  $^{13}\text{C}$  NMR spectrum of model compound **12** from solution (Figure 9). The most downfield-shifted signal of cage **3** appears at  $\delta=161.1$  ppm for the imine carbon nuclei; this is comparable to the signal for the imine  $^{13}\text{C}$  nucleus of model compound **12** ( $\delta=162.7$  ppm). Furthermore, in the typical carbonyl region of  $\delta=180\text{--}220$  ppm, no succinct signal is detected. Also, the range of aromatic signals of **3** between  $\delta=$

110 and 160 ppm correlates well with that of model compound **12**. The signals of the bridgehead  $^{13}\text{C}$  nuclei of **3** appear at  $\delta=53\text{--}55$  and 32–33 ppm, which is in the same region as the bridgehead  $^{13}\text{C}$  nuclei of **12** ( $\delta=55.6$  and 32.2 ppm).

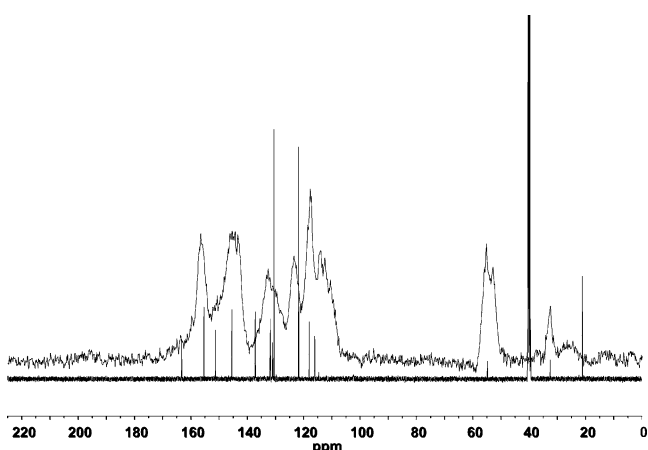


**Figure 9.** Comparison of the  $^{13}\text{C}$  CP MAS NMR spectrum of **3** (top) with the  $^{13}\text{C}$  NMR spectrum of model compound **12** (bottom) in  $[\text{D}_6]\text{DMSO}$  at 125 MHz.

Also, by IR spectra, structural analogy can be proven. The IR spectrum of **3** shows the same significant bands at  $\tilde{\nu}=1619$  and  $1596\text{ cm}^{-1}$  to those of compound **12** ( $\tilde{\nu}=1618$  and  $1596\text{ cm}^{-1}$ ) for the strong C=N stretching band (see the Supporting Information). However, a small shoulder can be detected at  $\tilde{\nu}\approx 1650\text{ cm}^{-1}$ , which might be assigned to partly cleaved imine bonds to the corresponding aldehyde and amine units under the conditions for the preparation of the IR sample (the signal for the aldehyde precursor resonates at  $\tilde{\nu}=1649\text{ cm}^{-1}$ ); this provides a clue for the reason behind the instability of the isolated cage compound (see also discussion above).

The porosity of cage compound **3** was studied by gas sorption experiments with various gases at different temperatures. Prior to gas sorption experiments, compound **3** was investigated by thermogravimetric analysis (TGA), which suggested thermal stability up to  $400^\circ\text{C}$  (see the Supporting Information).

After thermal activation for 3 h at  $200^\circ\text{C}$  in high vacuum ( $2.6\times 10^{-2}$  mbar), the nitrogen sorption of **3** was measured at 77 K (Figure 10). The isotherm has a typical type I shape, which is characteristic for microporous materials, and shows a small but pronounced hysteresis between adsorption and desorption.<sup>[50]</sup> The derived specific surface area was found to be 1014 (BET model) or  $1122\text{ m}^2\text{ g}^{-1}$  (Langmuir model) with a micropore volume of  $V_{\text{micro}}=0.31\text{ cm}^3\text{ g}^{-1}$  calculated by the *t*-plot method.<sup>[51]</sup> QSDFT calculations<sup>[52]</sup> showed a narrow pore size distribution with a sharp maximum at 1.22 nm (Figure 10, inset) in the microporous regime ( $\text{N}_2$  adsorption branch at 77 K, cylindrical/spherical pores, carbon material, fitting error 0.431%). This value is in good agreement with the diameter of a calculated sphere fitting to the void of **3** ( $d=1.31$  nm, see Scheme 1). In comparison, by non-localised density functional theory (NLDF) calculations ( $\text{N}_2$  adsorption branch at 77 K, cy-

lindrical/spherical pores, silicon material) with  $d = 1.11$  nm, a smaller pore diameter was found. However, although the fitting error (0.310%) is smaller than that for QSDFTone has to keep in mind that the QSDFT method was developed for amorphous materials.<sup>[52]</sup> All gas sorption data are reproducible, for example, second and third batches of cage compound 3 gave BET surface areas of 1006 and 979 m<sup>2</sup> g<sup>-1</sup>, respectively, and the derived pore dimensions are also similar to those discussed above.

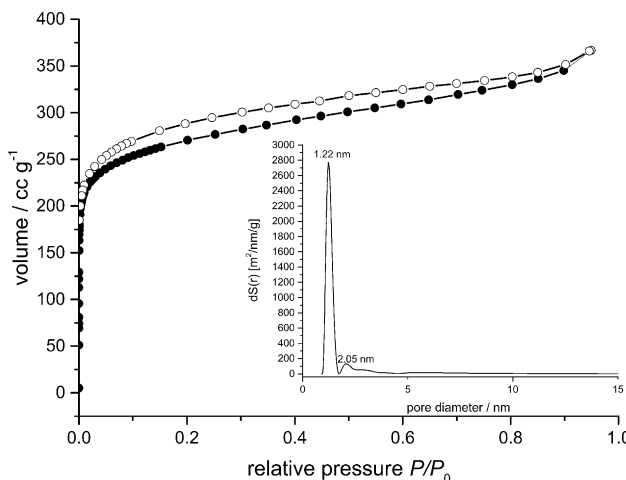


**Figure 10.** Nitrogen sorption isotherm at 77 K. ●: adsorption, ○: desorption. Inset: quenched solid density functional theory (QSDFT) pore size distribution.

Powder X-ray diffraction (PXRD) measurements of the material after gas sorption revealed the amorphous character of the sample (see the Supporting Information); this suggested that the QSDFT method might be better applicable to describe the pore structure of the material and indeed fit better to the pore dimensions of the molecular model. It should be mentioned that describing the pore structure of amorphous materials derived from organic cages by theoretical models is challenging and, although some progress has been made by the groups of McKeown<sup>[23]</sup> and Cooper,<sup>[53]</sup> it should be mentioned that there is still a significant difference between experimental and theoretical gas sorption properties.

In comparison to other amorphous porous materials based on discrete molecular units, the high surface area of 1014 m<sup>2</sup> g<sup>-1</sup> is, to the best of our knowledge, one of the highest values, reported so far.<sup>[12b,d,13a,36,54]</sup> Therefore, we also investigated the adsorption of other gases such as hydrogen, carbon dioxide and methane.

The material adsorbs 7.29 mmol g<sup>-1</sup> of H<sub>2</sub> at 77 K and 1 bar, which correlates to 1.47 wt%, and is comparable to co-crystallised cages CC1S and CC3R (7.6 mmol g<sup>-1</sup>, 1.52 wt%) reported by Cooper et al.<sup>[13f]</sup> and slightly higher than the value for [4+6]-tBu cage (5.6 mmol g<sup>-1</sup>, 1.13 wt%).<sup>[12d]</sup> but lower than, for example, the values for CC5R<sup>[13f]</sup> (Table 1) or TTBI (10.8 mmol g<sup>-1</sup>, 2.2 wt%).<sup>[55]</sup> At higher temperatures, the uptake of hydrogen was almost negligible: 0.17 mmol g<sup>-1</sup> (0.034 wt%) at 273 K and 0.14 mmol g<sup>-1</sup> (0.028 wt%) at 263 K.

The selective adsorption of carbon dioxide from nitrogen or methane is an important topic to remove CO<sub>2</sub> pre- or post-combustive.<sup>[56]</sup> Therefore, we measured the adsorption of those gases and calculated selectivities for mixtures based on Henry's law.<sup>[57]</sup> At 263 K and 1 bar, 4.82 mmol g<sup>-1</sup> (21.2 wt%) of carbon dioxide is adsorbed, and at 273 K and 1 bar 4.14 mmol g<sup>-1</sup> (18.2 wt%) of carbon dioxide is adsorbed. The high amounts of CO<sub>2</sub> adsorbed are, so far, unprecedented for materials based on discrete molecules (here the highest reported value is 3.4 mmol g<sup>-1</sup> for the [4+6] exo-cage compound published by our group).<sup>[12b]</sup> However, the value is still substantially lower than that, for example, for Mg-MOF-74<sup>[58]</sup> (8.61 mmol g<sup>-1</sup>; 37.8 wt% at 298 K and 1 bar) or the amorphous organic framework material BILP-4<sup>[59]</sup> (24 wt% at 273 K and 1 bar). In contrast to the high amounts of carbon dioxide, at 273 K, only 1.27 mmol g<sup>-1</sup> (2.08 wt%) of methane was adsorbed and, at 263 K, 1.64 mmol g<sup>-1</sup> (2.6 wt%) of methane was adsorbed, which was a higher uptake than that for most crystalline cage compounds, except a mixture of CC1S and CC3R (Table 1).

By fitting the Langmuir-Freundlich equation to the obtained isotherms at 263 and 273 K, parameters for the Clausius-Clapryon equation<sup>[60]</sup> were obtained to calculate the isosteric heat of adsorption for carbon dioxide and methane, depending on the uptake (see the Supporting Information). The obtained differences in heats of adsorption were similar. At 0.01, 0.1 or 1 mmol g<sup>-1</sup> of uptake, the heats of adsorption were  $Q_{st} =$

**Table 1.** Comparison of gas sorption data for cage compound 3 with those of other cage compounds published previously.<sup>[a]</sup>

Compound	Phase	SA <sub>BET</sub> [m <sup>2</sup> g <sup>-1</sup> ] N <sub>2</sub> , 77 K	SA <sub>Langmuir</sub> [m <sup>2</sup> g <sup>-1</sup> ] N <sub>2</sub> , 77 K	V <sub>Mirco</sub> [cm <sup>-3</sup> g <sup>-1</sup> ]	CO <sub>2</sub> [mmol g <sup>-1</sup> ] at 1 bar, 273 K	CH <sub>4</sub> [mmol g <sup>-1</sup> ] at 1 bar, 273 K	H <sub>2</sub> [mmol g <sup>-1</sup> ] at 1 bar, 77 K	Ref.
3	amorphous	1014	1122	0.31	4.1 (18.2 wt%)	1.3 (2.08 wt%)	7.3 (1.47 wt%)	this work
[4+6]-tBu	crystalline	2071	2327	0.77	2.7 (11.9 wt%)	0.7 (1.12 wt%)	5.6 (1.13 wt%)	[12d, 20]
[4+6]-exo	amorphous	919	1037	0.30	3.4 (15.0 wt%)	0.7 (1.12 wt%)	4.7 (0.94 wt%)	[12b]
[2+3]cage	crystalline	744	835	0.26	2.7 (11.9 wt%) <sup>[b]</sup>	0.7 (1.12 wt%) <sup>[b]</sup>	n.d.	[12c]
[2+3]-extend	crystalline	30	204	— <sup>[c]</sup>	3.3 (14.5 wt%) <sup>[b]</sup>	0.3 (0.48 wt%) <sup>[b]</sup>	n.d.	[12c]
CC1S/CC3R (1:1)	crystalline	437	n.d.	n.d.	3.3 (14.5 wt%) <sup>[d]</sup>	1.7 (2.73 wt%) <sup>[e]</sup>	7.6 (1.52 wt%) <sup>[f]</sup>	[13f]
CC5-R	crystalline	1333	n.d.	n.d.	3.1 (13.6 wt%) <sup>[g]</sup>	n.d.	8.5 (1.71 wt%) <sup>[g]</sup>	[13f]
Noria	crystalline	350 <sup>[h]</sup>	n.d.	0.13	2.5 (11.0 wt%) <sup>[i]</sup>	n.d.	n.d.	[9]

[a] SA = surface area. [b] Measured at 298 K. [c] The t-plot analysis revealed that the observed surface was not derived from micropores. [d] Determined at 1.2 bar. [e] Determined at 0.85 bar. [f] Determined at 1.17 bar. [g] Determined at 1.1 bar. [h] Determined with CO<sub>2</sub>. [i] Determined at 298 K at 30 bar.

–34.47, –28.43 and –22.92 kJ mol<sup>–1</sup>, respectively, for methane or  $Q_{st} = –32.64$ , –27.59 and –22.44 kJ mol<sup>–1</sup>, respectively, for carbon dioxide. It is known that a virial method gives more reliable results at lower coverage due to the incorrect fitting of the Langmuir–Freundlich equation to the low-pressure regime. By applying the virial method, the heats of adsorption for zero coverage have been calculated to be  $Q_{st} = –24.23$  kJ mol<sup>–1</sup> for carbon dioxide and  $Q_{st} = –26.46$  kJ mol<sup>–1</sup> for methane. Both calculation methods show that neither gas has a higher physical affinity to cage compound **3**. This is also represented with the low Henry's law selectivities of carbon dioxide over methane. The Henry's law selectivity was calculated by dividing the Henry's law constants of the gases at a defined temperature. To calculate the Henry's law constants, a non-linear Tóth equation was fitted to the isotherms and the obtained parameters were used in Henry's law (see the Supporting Information).<sup>[57]</sup> This method should be more reliable than giving the selectivities as a ratio of the maximum uptakes of individual gases (the so-called ideal selectivity). The mentioned selectivity of carbon dioxide over methane was found to be  $S = 7.10$  at 263 K and  $S = 7.67$  at 273 K. A high Henry's law selectivity was found for carbon dioxide over hydrogen ( $S = 134$  at 263 K and  $S = 105$  at 273 K) and for a mixture of CO<sub>2</sub> and N<sub>2</sub> selectivities of  $S = 40.1$  at 263 K and  $S = 33.7$  at 273 K for carbon dioxide over nitrogen were calculated. These are, for instance, higher than those reported recently for ZIF-300 and ZIF-302 with  $S = 17$  or 22,<sup>[61]</sup> or NOTT-202 with  $S = 27.3$ <sup>[62]</sup>

## Conclusion

A synthetic route to triptycene tris-salicylaldehyde **1** was developed, and used as a precursor in the synthesis of a molecular porous cube, which formed an amorphous porous material with a very high BET surface area (1014 m<sup>2</sup> g<sup>–1</sup>) and a good Henry selectivity for the adsorption for CO<sub>2</sub> over N<sub>2</sub> of  $S = 33.7$ . More importantly than extraordinarily high selectivities, the materials showed high selectivities in combination with high amounts of adsorbed gas (18.2 wt % of CO<sub>2</sub> at 273 K and 1 bar); this might be more feasible for applications in gas separation.<sup>[56]</sup>

In addition to being a reactant for cubic cages, tris-salicylaldehyde **1** is a versatile precursor to synthesise discrete trinuclear salphene complexes,<sup>[54a,63]</sup> and metal-assisted salphene organic frameworks,<sup>[64]</sup> which are currently under investigation in our laboratories.

## Experimental Section

### General

NMR spectra were recorded on Bruker DRX 500 (<sup>1</sup>H NMR: 500 MHz; <sup>13</sup>C NMR: 125 MHz), DRX 400 (<sup>1</sup>H NMR: 400 MHz; <sup>13</sup>C NMR: 100 MHz) or DRX 300 (<sup>1</sup>H NMR: 300 MHz) spectrometers at 298 K, unless otherwise mentioned. Chemical shifts ( $\delta$ ) were given in ppm and were calibrated with residual non-deuterated solvent signals (CDCl<sub>3</sub>:  $\delta_H = 7.26$  ppm,  $\delta_C = 77.0$  ppm; [D6]DMSO:  $\delta_H = 2.50$  ppm,  $\delta_C = 39.5$  ppm) as internal standards. The <sup>13</sup>C CP-MAS NMR spectra were measured on a standard-bore Bruker Avance III 500.13 MHz

spectrometer equipped with a 4 mm <sup>1</sup>H/X CP-MAS probe. The Bruker standard pulse program cp was used with a rotational frequency of 15 kHz, a ramped contact time of 2 ms, a recycle delay of 4 s and a spinal 64 proton broadband decoupling with a radio-frequency (RF) field of 100 kHz. The spectrum was referenced to external adamantane ( $\delta = 38.48$  ppm). CI mass spectrometry was performed with a Finnigan MAT SSQ-7000 instrument. MALDI-TOF mass spectra were recorded with a Bruker Daltonics Reflex III spectrometer and HRMS experiments were carried out on a Fourier-transform ion cyclotron resonance (FT-ICR) mass spectrometer solariX (Bruker Daltonik GmbH, Bremen, Germany) equipped with a 7.0 T superconducting magnet and interfaced to an Apollo II Dual ESI/MALDI source. Dithranol or *trans*-2-[3-(4-*tert*-butylphenyl)-2-methyl-2-propenylidene]malononitrile (DCTB) were used as matrices. IR spectra were recorded as KBr pellets with a PerkinElmer FTIR Spectrum 2000 spectrometer or on a Bruker Lumos spectrometer on a Ge ATR crystal. Melting points (uncorrected) were recorded on a Büchi B-545 or B-540 apparatus. Elemental analyses were recorded on an Elementar Vario EL instrument (Ulm University and Microanalytical Laboratory of the University of Heidelberg). TGA results were measured on a Mettler Toledo TGA/SDTA 851 instrument with a heating rate of 10 °C min<sup>–1</sup> and a nitrogen flow of 50 mL min<sup>–1</sup>, or were recorded on a Mettler-Toledo TGA/DSC1 instrument with a TGA/DSC-Sensor 1100 equipped with a MX1 balance (Mettler-Toledo) and a GC100 gas control box for nitrogen supply. TGA samples were measured in 70 µL Al<sub>2</sub>O<sub>3</sub> crucibles. All measurements were carried out under a flow of nitrogen (20 mL min<sup>–1</sup>). The surface area and porosity of **3** were characterised by nitrogen adsorption and desorption analysis at 77.35 K with an autosorb computer-controlled surface analyser (AUTOSORB-iQ, Quantachrome). The sample was degassed at 200 °C (3 h) before being analysed. The BET surface area was calculated by assuming a value of 0.162 nm<sup>2</sup> for the cross-sectional area of the nitrogen molecules in the pressure range  $P/P_0 = 0.01$ –0.1. The QSDFT model and isotherm data were used to calculate the pore size distribution (Kernel N2-carb.gai). Crystal structure analysis was accomplished on an Agilent SuperNova Atlas (Dual Source) diffractometer with a copper source ( $\lambda(CuK\alpha) = 1.54178$  Å) as well as on Bruker APEX-II Quazar and Bruker APEX I diffractometers with molybdenum sources ( $\lambda(MoK\alpha) = 0.71073$  Å). The structures were solved and refined with SHELXTL 2008/4 software<sup>[65]</sup> and for absorption correction the SADABS 2012/1 software<sup>[66]</sup> was used. Powder diffraction was performed with a STOE Stadi P Ge(111)-monochromated copper radiation ( $\lambda(CuK\alpha) = 1.54060$  Å). The diffractograms were obtained with a Stoe linear PSD detector. Compound **3** was measured in a glass capillary ( $\varnothing = 0.5$  mm) as a sample container. Plastic sheets pre-coated with silica gel (Merck Si60 F<sub>254</sub>) were used for TLC. Glass columns packed with Merck silica 60 (mesh 40–60 µm) were used for flash-chromatography purification. All reagents and solvents were obtained from Fisher Scientific, Alfa Aesar, Sigma-Aldrich, ProLabo or VWR and were used without further purification unless otherwise noted. Triaminotriptycene **2**,<sup>[22]</sup> triflate **4** and 1,8-dimethoxyanthracene (**5**) were synthesised according to known procedures.<sup>[30,31]</sup> For the assignment of NMR spectroscopy signals, triptycene was seen as 9,10-dihydro-9,10[1,2]benzoanthracene.<sup>[67]</sup>

### Synthetic Procedures

**Compounds 6a and 6b:** 2-Methoxy-6-trimethylsilylphenyltrifluoromethane sulfonate (**4**; 4.00 g, 12.2 mmol) was added to a suspension of **5** (2.50 g, 10.5 mmol) and caesium fluoride (5.00 g, 32.9 mmol) in dry acetonitrile (160 mL). The mixture was stirred under argon for 40 h at room temperature. After removal of solvent by rotary evaporation, the residual yellow solid was washed

with water (250 mL), methanol (200 mL) and  $\text{CH}_2\text{Cl}_2$  (200 mL) to give of **6a** and **6b** as an inseparable mixture (1.86 g, 5.40 mmol, 51%) in a 2:1 ratio (determined by  $^1\text{H}$  NMR spectroscopy) as a white solid. M.p. 365 °C (dec);  $^1\text{H}$  NMR (500 MHz,  $[\text{D}_6]\text{DMSO}$ , 375 K):  $\delta$  = 7.06–7.02 (m, 9H; Ar-4,4',5,5',13',16-H), 6.95–6.92 (m, 9H; Ar-3,3',6,6',14',15-H), 6.69–6.68 (m, 11H; Ar-2,2',7,7',14,15', bridgehead-9'-H), 6.24 (s, 1H; bridgehead-9'-H), 5.85 (s, 1H; bridgehead-10'-H), 5.53 (s, 2H; bridgehead-10'-H), 3.84 ppm (s, 27H;  $\text{OCH}_3$ );  $^{13}\text{C}$  NMR (125 MHz,  $[\text{D}_6]\text{DMSO}$ , 375 K):  $\delta$  = 153.8 (Ar-C-OCH<sub>3</sub>), 147.9 (Ar-C-4a,10a,11), 147.2 (Ar-C-4a',10a'), 146.7 (Ar-C-12a'), 132.7 (Ar-C-8a',9a',11'), 132.4 (Ar-C-8a,9a,12), 125.4 (Ar-C-14'), 125.3 (Ar-C-3',6'), 125.2 (Ar-C-3,6,15), 116.1 (Ar-C-4,5,16), 116.0 (Ar-C-4',5',13'), 109.1 (Ar-C-2,7,14), 108.9 (Ar-C-2',7'), 108.8 (Ar-C-15'), 55.7 (Ar-C-1,8,13-OCH<sub>3</sub>), 55.6 (Ar-C-1',8'-OCH<sub>3</sub>), 55.5 (Ar-C-16'-OCH<sub>3</sub>), 53.1 (bridgehead-C-10), 46.2 (bridgehead-C-10'), 32.6 ppm (bridgehead-C-9'); IR (KBr pellet):  $\tilde{\nu}$  = 3435 (br, w), 3036 (w), 2999 (m), 2961 (m), 2938 (m), 2904 (m), 2835 (m), 2648 (w), 2590 (w), 2521 (w), 2332 (m), 2198 (w), 1993 (w), 1912 (w), 1822 (w), 1741 (w), 1655 (w), 1596 (s), 1583 (s), 1484 (s), 1439 (s), 1324 (m), 1275 (s), 1197 (m), 1160 (w), 1103 (s), 1092 (s), 1065 (s), 980 (m), 959 (w), 934 (w), 870 (w), 852 (w), 789 (s), 777 (m), 751 (s), 729 (s), 632 (w), 592 (m), 542 (w), 516 (w), 486 (w), 454 (w), 405 (w)  $\text{cm}^{-1}$ ; MS (Cl);  $m/z$  (%) = 373 (6), 346 (26), 345 (100) [M+H]<sup>+</sup>, 344 (51) [M]<sup>+</sup>, 313 (11); elemental analysis calcd (%) for C<sub>23</sub>H<sub>20</sub>O<sub>3</sub>: C 80.21, H 5.85; found: C 80.43, H 5.61.

By-products were isolated by removing the solvent from the  $\text{CH}_2\text{Cl}_2$  extract followed by column chromatography (SiO<sub>2</sub>, petroleum ether/ethyl acetate, 7:1) and recrystallisation of the isolated fractions from ethyl acetate.

**First fraction ( $R_f$  = 0.23):** **rac-6c** (930 mg, 2.70 mmol, 25%) as colourless crystals. M.p. 212–213 °C;  $^1\text{H}$  NMR (400 MHz,  $[\text{D}_6]\text{DMSO}$ ):  $\delta$  = 8.09 (s, 1H; Ar-11-H), 7.64 (s, 1H; Ar-6-H), 7.35–7.29 (m, 2H; Ar-8,9-H), 7.24 (dd,  $J$  = 7.8, 1.5 Hz, 1H; olefin-13-), 7.07 (dd,  $J$  = 7.7, 6.1 Hz, olefin-14-H), 7.01 (dd,  $J$  = 7.2, 1.1 Hz, 1H; Ar-4-H), 6.98–6.95 (m, 1H; Ar-3-H), 6.89 (dd,  $J$  = 7.0, 1.4 Hz, 1H; Ar-9-H), 6.72 (dd,  $J$  = 8.1, 1.0 Hz, Ar-2-H), 5.22 (dd,  $J$  = 6.1, 1.4 Hz, 1H; bridgehead-5-H), 3.92 (s, 3H;  $\text{OCH}_3$ ), 3.84 (s, 3H;  $\text{OCH}_3$ ), 3.75 ppm (s, 3H;  $\text{OCH}_3$ );  $^{13}\text{C}$  NMR (100 MHz,  $[\text{D}_6]\text{DMSO}$ ):  $\delta$  = 155.0 (Ar-C-10), 154.5 (Ar-C-1), 147.0 (Ar-C-4a), 143.2 (Ar-C-5a/11a), 142.3 (Ar-C-5a/11a), 137.7 (olefin-C-13), 137.1 (olefin-C-14), 131.6 (Ar-C-6a/12a), 131.4 (Ar-C-6a/12a), 126.5 (Ar-C-3), 126.1 (Ar-C-8), 121.8 (Ar-C-10a), 120.0 (Ar-C-6), 119.5 (Ar-C-7), 116.5 (Ar-C-4), 112.1 (Ar-C-11), 110.6 (Ar-C-2), 104.6 (Ar-C-9), 87.3 (Ar-C-12), 56.2 (Ar-C-1-OCH<sub>3</sub>), 55.5 (OCH<sub>3</sub>), 55.3 (OCH<sub>3</sub>), 48.9 ppm (bridgehead-C-5); IR (KBr pellet):  $\tilde{\nu}$  = 3436 (br, w), 3055 (w), 3000 (w), 2936 (m), 2833 (m), 2361 (w), 2342 (2), 1904 (w), 1725 (w), 1607 (w), 1587 (m), 1502 (w), 1477 (m), 1466 (m), 1439 (m), 1423 (w), 1369 (m), 1336 (m), 1267 (s), 1231 (m), 1201 (w), 1187 (w), 1128 (w), 1109 (w), 1065 (m), 1037 (m), 966 (w), 966 (w), 939 (w), 894 (w), 876 (w), 853 (w), 809 (w), 789 (w), 777 (s), 753 (m), 739 (w), 722 (w), 715 (w), 685 (m), 635 (w), 601 (w), 573 (w), 498 (w), 431  $\text{cm}^{-1}$  (w); MS (El);  $m/z$  (%) = 346 (5), 345 (24) [M+H]<sup>+</sup>, 344 (100) [M]<sup>+</sup>, 331 (10), 330 (56), 329 (15), 315 (14), 314 (36), 313 (21), 312 (11), 302 (7), 301 (6), 300 (6), 299 (8), 298 (10), 297 (7), 296 (7), 295 (5), 286 (5), 285 (5), 284 (5), 254 (5); elemental analysis calcd (%) for C<sub>23</sub>H<sub>20</sub>O<sub>3</sub>: C 80.21, H 5.85; found: C 80.02, H 5.84.

**Second fraction ( $R_f$  = 0.15):** **rac-6d** (154 mg, 0.34 mmol, 3%) as a white solid after drying in high vacuum. M.p. 347–348 °C (dec);  $^1\text{H}$  NMR (400 MHz,  $[\text{D}_6]\text{DMSO}$ ):  $\delta$  = 7.49 (s, 1H; Ar-13-H), 7.19 (s, 1H; Ar-6-H), 7.15 (dd,  $J$  = 7.6, 1.4 Hz, 2H; olefin-16,18-H), 6.97–6.93 (m, 2H; olefin-15,17-H), 6.92–6.86 (m, 4H; Ar-3,4,8,9-H), 6.65 (dd,  $J$  = 7.7, 1.4 Hz, 2H; Ar-2,10-H), 4.99 (dd,  $J$  = 6.0, 1.2 Hz, 2H; bridgehead-5,7-H), 3.76 (s, 6H;  $\text{OCH}_3$ ), 3.73 ppm (s, 6H;  $\text{OCH}_3$ );  $^{13}\text{C}$  NMR (100 MHz,  $[\text{D}_6]\text{DMSO}$ ):  $\delta$  = 153.9 (Ar-C-1,11), 147.9 (Ar-C-4a,7a), 143.2

(Ar-C-5a,6a), 141.0 (Ar-C-12a,13a), 137.7 (olefin-C-15,17/16,18), 137.4 (olefin-C-15,17/16,18), 132.9 (Ar-C-11a,14a), 125.1 (Ar-C-3,9/4,8), 117.0 (Ar-C-6), 115.8 (Ar-C-3,9/4,8), 112.4 (Ar-C-13), 110.8 (Ar-C-2,10), 87.7 (bridgehead-C-12,14), 56.2 (Ar-OCH<sub>3</sub>), 54.5 (bridgehead-OCH<sub>3</sub>), 49.1 ppm (bridgehead-C-5,7); IR (KBr pellet):  $\tilde{\nu}$  = 3436 (br, w), 3066 (w), 2961 (m), 2935 (m), 2833 (m), 1613 (w), 1583 (m), 1478 (s), 1439 (w), 1329 (m), 1267 (s), 1227 (w), 1212 (w), 1190 (w), 1141 (m), 1120 (w), 1105 (w), 1067 (m), 1030 (m), 942 (w), 906 (w), 793 (w), 778 (w), 755 (w), 735 (w), 698 (w), 668 (m), 636 (w), 588 (w), 564  $\text{cm}^{-1}$  (w); MS (El);  $m/z$  (%): 452 (7), 451 (32) [M+H]<sup>+</sup>, 450 (100) [M]<sup>+</sup>, 439 (5), 438 (11), 437 (21), 436 (33), 435 (7), 422 (5), 421 (12), 420 (19), 419 (23), 418 (10), 417 (6), 407 (6), 406 (8), 405 (14), 404 (17), 403 (15), 402 (8), 401 (7), 400 (5), 390 (5), 389 (7), 388 (9), 387 (9), 386 (7), 385 (5), 384 (5), 375 (6), 374 (6), 373 (6), 372 (7), 371 (6), 370 (6), 361 (5), 358 (5), 356 (5); elemental analysis calcd (%) for C<sub>30</sub>H<sub>26</sub>O<sub>4</sub>·1.5H<sub>2</sub>O: C 75.45, H 6.12; found: C 75.17, H 5.76.

**Compounds 7a and 7b:** Boron tribromide in  $\text{CH}_2\text{Cl}_2$  (1 M, 40 mL, 40 mmol) was added dropwise to a suspension of **6a/b** (2:1 ratio; 3.00 g, 8.71 mmol) in dry  $\text{CH}_2\text{Cl}_2$  (30 mL) at 0 °C. After complete addition, the vine-red solution was allowed to stir overnight at room temperature. The mixture was cooled again to 0 °C and ice (150 g) and water (150 mL) were added. The layers were separated and the residual suspension was extracted with ethyl acetate (3 × 300 mL). The combined organic layer was washed with water (2 × 200 mL) and brine (200 mL), and dried over sodium sulfate. After removal of the solvent in vacuum, compounds **7a** and **7b** (2.56 g, 8.46 mmol, 97%) remained as a white solid in a 2:1 mixture (determined by  $^1\text{H}$  NMR spectroscopy). M.p. >410 °C (dec at 350 °C);  $^1\text{H}$  NMR (400 MHz,  $[\text{D}_6]\text{DMSO}$ ):  $\delta$  = 9.41–9.36 (m, 9H; OH), 6.86–6.83 (m, 9H; Ar-4,4',5,5',16,13'-H), 6.77–6.71 (m, 9H; Ar-3,3',6,6',15,14'-H), 6.50–6.46 (m, 11H; Ar-2,2',7,7',14,15', bridgehead-9-H), 6.10 (s, 1H; bridgehead-9'-H), 5.70 (s, 1H; bridgehead-10'-H), 5.35 ppm (2H; bridgehead-10-H);  $^{13}\text{C}$  NMR (100 MHz,  $[\text{D}_6]\text{DMSO}$ ):  $\delta$  = 151.9 (Ar-C-16'), 151.8 (Ar-C-1',8'), 151.7 (Ar-C-1,8,13), 148.4 (Ar-C-4a,10a,11), 147.9 (Ar-C-4a',10a'), 147.7 (Ar-C-12'), 131.5 (Ar-C-11'), 131.3 (Ar-C-8a',9a'), 131.2 (Ar-C-8a,9a,12), 125.3 (Ar-C-14'), 125.2 (Ar-C-3',6'), 125.0 (Ar-C-3,6,15), 114.8 (Ar-C-4,4',5,5',16,13'), 112.5 (Ar-C-2,2',7,7',14,15'), 53.7 (bridgehead-C-10), 46.7 (bridgehead-C-10'), 33.1 ppm (bridgehead-C-9); IR (KBr pellet):  $\tilde{\nu}$  = 3306 (s), 2975 (w), 2847 (w), 2716 (w), 1889 (w), 1819 (w), 1601 (s), 1474 (s), 1459 (s), 1389 (m), 1389 (w), 1323 (w), 1296 (w), 1255 (s), 1224 (w), 1189 (w), 1160 (w), 1079 (w), 1059 (w), 1037 (w), 975 (w), 862 (w), 786 (w), 772 (w), 758 (m), 753 (m), 726 (s), 625 (w), 569 (w), 545 (w), 471 (w), 400 (w)  $\text{cm}^{-1}$ ; MS (Cl);  $m/z$  (%): 331 (20), 304 (5), 303 (100) [M+H]<sup>+</sup>, 302 (24) [M]<sup>+</sup>; elemental analysis calcd (%) for C<sub>20</sub>H<sub>14</sub>O<sub>3</sub>: C 79.46, H 4.67; found: C 79.38, H 4.55.

**Compound 8a:** A 2:1 mixture of **7a** and **7b** (150 mg, 0.50 mmol) was suspended in dry N-methylimidazole (2 mL) and stirred for 30 min at room temperature under argon in a screw-capped vial. Freshly distilled capronyl chloride (2 mL) was added to the resulting bright-red solution and the mixture was stirred for 16 h at room temperature. The accrued suspension was poured into cold water (50 mL); extracted with  $\text{CH}_2\text{Cl}_2$  (3 × 40 mL); and the combined organic layer was washed with dilute hydrochloric acid (1 M, 2 × 40 mL), a saturated solution of sodium hydrogen carbonate (50 mL), water (2 × 50 mL) and brine (50 mL). After being dried over sodium sulfate,  $\text{CH}_2\text{Cl}_2$  was removed in vacuo and n-pentane (10 mL) was added to the resulting brown oil. Colourless crystals were obtained overnight and isolated by suction filtration to give **8a** (98 mg, 0.16 mmol, 32%). M.p. 139 °C;  $^1\text{H}$  NMR (400 MHz, CDCl<sub>3</sub>):  $\delta$  = 7.25 (d, 3H; Ar-4,5,16-H), 7.00 (dd,  $J$  = 8.1, 7.4 Hz, 3H; Ar-3,6,15-H), 6.79 (dd,  $J$  = 8.2, 0.8 Hz, 3H; Ar-2,7,14-H), 5.82 (s, 1H; bridgehead-9-H), 5.50 (s, 1H; bridgehead-10-H), 2.64 (t, 6H;

$\text{COCH}_2\text{C}_4\text{H}_9$ ), 1.91–1.84 (m, 6H;  $\text{COCH}_2\text{CH}_2\text{C}_3\text{H}_7$ ), 1.48–1.40 (m, 12H;  $\text{COC}_2\text{H}_4\text{CH}_2\text{CH}_2\text{CH}_3$ ), 0.97 ppm (t,  $J=7.1$  Hz, 9H;  $\text{COC}_4\text{H}_8\text{CH}_3$ );  $^{13}\text{C}$  NMR (100 MHz,  $\text{CDCl}_3$ ):  $\delta=171.3$  (C=O), 147.7 (Ar-C-1,8,13) 145.9 (Ar-C-4a,10a,11), 134.9 (Ar-C-8a,9a,12), 126.9 (Ar-C-3,6,15), 121.3 (Ar-C-4,5,16), 119.4 (Ar-C-2,7,14), 54.0 (bridgehead -C-10), 36.3 (bridgehead -C-9), 34.5 (Alk-C-1,1',1''), 31.7 (Alk-C-3,3',3''), 25.0 (Alk-C-2,2',2''), 22.6 (Alk-C-4,4',4''); IR (KBr pellet):  $\tilde{\nu}=3500$  (br, w), 3409 (w), 3062 (w), 3019 (w), 2952 (m), 2939 (m), 2870 (m), 2732 (w), 2359 (w), 2342 (w), 1946 (w), 1912 (w), 1759 (s), 1609 (w), 1594 (w), 1548 (w), 1474 (m), 1438 (w), 1421 (w), 1376 (m), 1317 (m), 1293 (w), 1232 (s), 1164 (s), 1150 (s), 1113 (m), 1060 (w), 1029 (w), 974 (w), 924 (w), 887 (w), 855 (w), 801 (m), 752 (m), 726 (m), 623 (w), 598 (w), 569 (w), 540 (w), 437 (w), 410  $\text{cm}^{-1}$  (w); MS (Cl);  $m/z$  (%): 626 (10), 599 (5), 598 (33)  $[\text{M}+\text{H}]^+$ , 596 (25), 528 (5), 527 (8), 501 (5), 500 (31), 499 (100), 498 (65), 402 (12), 401 (9), 400 (20), 303 (6), 302 (25), 301 (5), 99 (6); elemental analysis calcd (%) for  $\text{C}_{38}\text{H}_{44}\text{O}_6$ : C 76.48, H 7.43; found: C 76.53, H 7.35.

**Compounds 9a and 9b:** A 2:1 mixture of **7a** and **7b** (2.91 g, 9.63 mmol) and *N*-methylimidazole (40 mL) were stirred for 2 h at room temperature in dry  $\text{CH}_2\text{Cl}_2$  (150 mL). The resulting bright-red suspension was cooled to 0 °C and freshly distilled acetyl chloride (40 mL) was added very slowly. After addition, cooling was removed and the mixture was allowed to stir overnight at room temperature. Cold water (150 mL) was added, the layers were separated and the aqueous layer was extracted with  $\text{CH}_2\text{Cl}_2$  (4×200 mL). The combined organic layer was washed with dilute hydrochloric acid (1 M, 2×250 mL), a saturated solution of sodium hydrogen carbonate (250 mL), water (2×250 mL) and brine (250 mL). After drying over sodium sulfate,  $\text{CH}_2\text{Cl}_2$  was removed by rotary evaporation. The residual solid was re-dissolved in  $\text{CH}_2\text{Cl}_2$  (100 mL), a layer of the same amount of *n*-pentane was added, and the mixture was kept at room temperature overnight. The resulting crystals were separated by suction filtration. This was performed twice to give pure isomer **9a** (1.79 g, 4.18 mmol, 43%) as colourless crystals after drying in high vacuum ( $6.3 \times 10^{-2}$  bar, 125 °C). M.p. 322 °C (dec);  $^1\text{H}$  NMR (400 MHz,  $[\text{D}_6]\text{DMSO}$ ):  $\delta=7.40$  (d,  $J=7.3$  Hz, 3H; Ar-4,5,16-H), 7.08 (t,  $J=7.8$  Hz, 3H; Ar-3,6,15-H), 6.84 (d,  $J=8.1$  Hz, 3H; Ar-2,7,14-H), 5.89 (s, 1H; bridgehead-9-H), 5.60 (s, 1H; bridgehead-10-H), 2.43 ppm (s, 9H;  $\text{COCH}_3$ );  $^{13}\text{C}$  NMR (100 MHz,  $[\text{D}_6]\text{DMSO}$ ):  $\delta=168.6$  (C=O), 147.6 (Ar-C-1,8,13) 145.5 (Ar-C-4a,10a,11), 134.6 (Ar-C-8a,9a,12), 126.4 (Ar-C-3,6,15), 121.6 (Ar-C-4,5,16), 119.4 (Ar-C-2,7,14), 52.0 (bridgehead-C-10), 35.7 (bridgehead-C-9), 20.4 ppm ( $\text{COCH}_3$ ); IR (KBr pellet):  $\tilde{\nu}=3435$  (br, w), 3063 (w), 3015 (w), 2932 (w), 2342 (w), 1773 (s), 1611 (w), 1593 (w), 1471 (m), 1438 (w), 1373 (m), 1209 (s), 1169 (s), 1076 (m), 1037 (m), 1019 (w), 973 (w), 905 (w), 879 (w), 863 (w), 847 (w), 798 (w), 772 (w), 751 (w), 741 (w), 722 (w), 696 (w), 683 (w), 667 (w), 596 (w), 543 (w), 505 (w), 478 (w), 415  $\text{cm}^{-1}$  (w); MS (El);  $m/z$  (%): 429 (16)  $[\text{M}+\text{H}]^+$ , 428 (13)  $[\text{M}]^+$ , 388 (25), 387 (100), 386 (16), 373 (7), 345 (6), 344 (10), 302 (7); elemental analysis calcd (%) for  $\text{C}_{26}\text{H}_{20}\text{O}_6$ : C 72.89, H 4.71; found: C 72.70, H 4.79.

The mother liquor of the filtration was freed from solvent by rotary evaporation and the residual solid was separated by column chromatography ( $\text{SiO}_2$ , chloroform/ethyl acetate, 99:1) to give **9b** (783 mg, 1.83 mmol, 19%).  $R_f=0.75$  (chloroform/ethyl acetate, 1:1) as the first fraction; m.p. 273 °C;  $^1\text{H}$  NMR (400 MHz,  $[\text{D}_6]\text{DMSO}$ ):  $\delta=7.35$  (d,  $J=7.3$  Hz, 3H; Ar-4,5,13-H), 7.06 (t,  $J=7.7$  Hz, 3H; Ar-3,6,14-H), 6.82 (d,  $J=8.1$  Hz, 3H; Ar-2,7,15-H), 5.82 (s, 1H; bridgehead-9-H), 5.65 (s, 1H; bridgehead-10-H), 2.48 (s, 3H; Ar-16-COCH<sub>3</sub>), 2.46 ppm (s, 6H; Ar-1,8-COCH<sub>3</sub>);  $^{13}\text{C}$  NMR (100 MHz,  $[\text{D}_6]\text{DMSO}$ ):  $\delta=169.4$  (Ar-C-16-COCH<sub>3</sub>), 169.0 (Ar-C-1,8-COCH<sub>3</sub>), 146.7 (Ar-C-1,8,16), 145.6 (Ar-C-12), 145.5 (Ar-C-4a,10a), 137.1 (Ar-C-8a,9a,11), 135.9 (Ar-C-3,6,14), 126.2 (Ar-C-3,6), 126.2 (Ar-C-15), 122.2 (Ar-C-13), 121.8 (Ar-

C-4,5), 119.4 (Ar-C-2,7,15), 46.7 (bridgehead-C-10), 41.4 (bridgehead-C-9), 20.8 (Ar-C-16-COCH<sub>3</sub>), 20.6 ppm (Ar-C-1,8-COCH<sub>3</sub>); IR (KBr pellet):  $\tilde{\nu}=3445$  (br, w), 3062 (w), 3018 (w), 3001 (w), 2935 (w), 2419 (w), 2051 (w), 1926 (w), 1763 (s), 1612 (w), 1610 (w), 1586 (w), 1472 (m), 1439 (w), 1372 (m), 1211 (s), 1164 (m), 1072 (w), 1033 (m), 979 (w), 909 (w), 901 (w), 894 (w), 878 (w), 851 (w), 793 (w), 769 (w), 746 (w), 732 (w), 722 (w), 679 (w), 668 (w), 595 (w), 566 (w), 548 (w), 530 (w), 480 (w), 445 (w), 411  $\text{cm}^{-1}$  (w); MS (Cl);  $m/z$  (%): 430 (11), 429 (45)  $[\text{M}+\text{H}]^+$ , 428 (31)  $[\text{M}]^+$ , 415 (10), 388 (24), 387 (100), 386 (32), 373 (9), 345 (9), 344 (16), 302 (19); elemental analysis calcd (%) for  $\text{C}_{26}\text{H}_{20}\text{O}_6$ : C 72.89, H 4.71; found: C 73.24, H 4.47.

A second fraction ( $R_f=0.68$ , 0.75; chloroform/ethyl acetate, 1:1) gave a mixture of **9b** (201 mg, 0.46 mmol, 5%) and **9a** (267 mg, 0.63 mmol, 6%); yields were determined by integration of the  $^1\text{H}$  NMR signals of the bridgehead protons.

From a third fraction ( $R_f=0.75$ ; chloroform/ethyl acetate, 1:1), more **9a** (562 mg, 1.31 mmol, 13%) was isolated with same analytical properties as the crystallized fraction. This gave an overall yield of **9a** of 56%.

**Compounds 10a and 10b:** In a screw-capped vial, a 2:1 mixture of **7a** and **7b** (150 mg, 0.50 mmol) and *N*-methylimidazole (2 mL) were stirred at room temperature for 30 min. A solution of benzoyl chloride (2 mL, 17.4 mmol) was added to the resulting bright-red solution and the mixture was stirred for 16 h at room temperature. The resulting suspension was poured into cold water (50 mL) and extracted with  $\text{CH}_2\text{Cl}_2$  (3×40 mL). The combined organic extract was washed with diluted hydrochloric acid (1 M, 2×40 mL), a saturated solution of sodium hydrogen carbonate (50 mL), water (2×50 mL) and brine (50 mL). After being dried over sodium sulfate,  $\text{CH}_2\text{Cl}_2$  was removed on a rotary evaporator. The residual off-white solid was dissolved in  $\text{CH}_2\text{Cl}_2$  (5 mL) and a layer of *n*-pentane was added. After crystallisation overnight, colourless crystals were isolated by suction filtration to give **10a** (130 mg, 0.21 mmol, 42%). M.p. 294 °C;  $^1\text{H}$  NMR (400 MHz,  $[\text{D}_6]\text{DMSO}$ ):  $\delta=7.74$  (dd,  $J=8.1$ , 1.0 Hz, 6H; Ph-2,6-H), 7.54–7.51 (m, 6H; Ar-4,5,16-H, Ph-4-H), 7.19–7.15 (m, 3H; Ar-3,6,15-H), 7.11 (t,  $J=7.8$  Hz, 6H; Ph-3,5-H), 6.99 (dd,  $J=8.1$ , 0.6 Hz, 3H; Ar-2,7,14-H), 6.03 (s, 1H; bridgehead-H-9), 5.94 ppm (s, 1H; bridgehead-H-10);  $^{13}\text{C}$  NMR (126 MHz, 360 K,  $[\text{D}_6]\text{DMSO}$ ):  $\delta=163.5$  (C=O), 147.4 (Ar-C-1,8,13), 145.2 (Ar-C-4a,10a,11), 134.4 (Ar-C-8a,9a,12), 132.9 (Ph-C-4), 128.7 (Ph-C-2,6), 128.0 (Ph-C-3,5/Ph-C-1), 127.9 (Ph-C-3,5/Ph-C-1), 126.0 (Ar-C-3,6,15), 121.1 (Ar-C-4,5,16), 119.0 (Ar-C-2,7,14), 52.2 (bridgehead-C-10), 35.5 ppm (bridgehead-C-9); IR (KBr pellet):  $\tilde{\nu}=3449$  (br, w), 3061 (w), 3032 (w), 2963 (w), 2344 (w), 1920 (w), 1740 (s), 1594 (w), 1473 (m), 1451 (w), 1314 (w), 1267 (s), 1245 (m), 1228 (s), 1171 (m), 1093 (s), 1060 (m), 1028 (w), 1016 (w), 1003 (w), 962 (w), 935 (w), 901 (w), 873 (w), 849 (w), 790 (w), 761 (w), 740 (w), 705 (s), 617 (w), 587 (w), 507 (w), 409  $\text{cm}^{-1}$  (m); MS (MALDI-TOF):  $m/z$  (%): 711.5 (12), 653.5 (44), 637.5 (100)  $[\text{M}+\text{Na}]^+$ , 614.5 (42)  $[\text{M}]^+$ ; elemental analysis calcd (%) for  $\text{C}_{26}\text{H}_{20}\text{O}_6$  (614.64): C 80.12, H 4.26; found: C 79.92, H 4.16.

The solvent was removed from the mother liquor and the residual solid was separated by column chromatography ( $\text{SiO}_2$ , chloroform) to give **10b** (47 mg, 0.08 mmol, 16%) as a colourless solid.  $R_f=0.37$ ; m.p. 287 °C;  $^1\text{H}$  NMR (400 MHz,  $[\text{D}_6]\text{DMSO}$ ):  $\delta=8.31$  (d,  $J=7.3$  Hz, 2H; Ph-2',6'-H), 8.03 (d,  $J=7.4$  Hz, 4H; Ph-2,6-H), 7.87–7.83 (m, 1H; Ph-4'-H), 7.74–7.66 (m, 4H; Ph-3',4,5'-H), 7.43 (t,  $J=7.9$  Hz, 6H; Ar-4,5-Ph-3,5-H), 7.34 (d,  $J=7.2$  Hz, 1H; Ar-13-H), 7.16–7.10 (m, 3H; Ar-3,6,14-H), 7.01 (t,  $J=8.5$  Hz, 3H; Ar-2,7,15-H), 5.90 (s, 1H; bridgehead-9-H), 5.74 ppm (s, 1H; bridgehead-10-H);  $^{13}\text{C}$  NMR (126 MHz, 360 K,  $[\text{D}_6]\text{DMSO}$ ):  $\delta=164.1$  (C=O), 163.8 (C=O), 146.3 (Ar-C-1,8,16), 145.4 (Ar-C-4a/10a/12), 145.2 (Ar-C-4a/10a/12), 145.2

(Ar-C-4a/10a/12), 136.5 (Ar-C-8a,9a/11), 135.4 (Ar-C-8a,9a/11), 133.5 (Ph-C-4'), 133.2 (Ph-C-4), 129.5 (Ph-C-2',6'), 129.0 (Ph-C-2,6), 128.5 (Ph-C-1/1'/3,5/3',5'), 128.3 (Ph-C-1/1'/3,5/3',5'), 128.2 (Ph-C-1/1'/3,5/3',5'), 126.0 (Ar-C-3,6), 125.9 (Ar-C-14), 121.5 (Ar-C-13), 121.4 (Ar-C-4,5), 118.9 (Ar-C-2,7,15), 47.1 (bridgehead-C-10), 41.7 ppm (bridgehead-C-9); IR (KBr pellet):  $\tilde{\nu}$  = 3444 (br, w), 3062 (w), 1924 (w), 1736 (s), 1600 (w), 1584 (w), 1471 (w), 1451 (w), 1265 (s), 1237 (s), 1234 (s), 1176 (m), 1091 (s), 1060 (m), 1027 (w), 874 (w), 858 (w), 782 (w), 764 (w), 738 (w), 705 (s), 685 (w), 589 cm<sup>-1</sup> (w); MS (MALDI-TOF): *m/z* (%): 653.5 (59), 637.5 (100) [M+Na]<sup>+</sup>, 614.5 (12) [M]<sup>+</sup>; elemental analysis calcd (%) for C<sub>41</sub>H<sub>26</sub>O<sub>6</sub>: C 77.84, H 4.46; found: C 78.11, H 4.30.

A second fraction gave further **10a** (40 mg, 0.065 mmol, 13%). The combined yield of **10a** was 55%.

**Compound 7a:** Compound **9a** (1.30 g, 3.03 mmol) was suspended in an mixture of ethanol/hydrochloric acid (1:2, v/v; 60 mL) and stirred for 16 h at 85 °C. The obtained white solid was filtered, washed with water (2 × 40 mL) and dried under high vacuum (5.1 × 10<sup>-1</sup> mbar, 125 °C) to give **7a** (820 mg, 2.71 mmol, 89%) as a white solid. M.p. > 410 °C; <sup>1</sup>H NMR (400 MHz, [D<sub>6</sub>]DMSO):  $\delta$  = 9.35 (s, 3H; OH), 6.85 (d, *J* = 7.1 Hz, 3H; Ar-4,5,16-H), 6.73 (t, *J* = 7.6 Hz, 3H; Ar-3,6,15-H), 6.49–6.47 (m, 4H; Ar-2,7,14-H, bridgehead-9-H), 5.35 ppm (s, 1H; bridgehead-10-H); <sup>13</sup>C NMR (100 MHz, [D<sub>6</sub>]DMSO):  $\delta$  = 151.7 (Ar-C-1,8,13), 148.4 (Ar-C-4a,10a,11), 131.1 (Ar-C-8a,9a,12), 125.0 (Ar-C-3,6,15), 114.8 (Ar-C-4,5,16), 112.5 (Ar-C-2,7,14), 53.7 (bridgehead-C-10), 33.0 ppm (bridgehead-C-9); IR (KBr pellet):  $\tilde{\nu}$  = 3308 (br, w), 3255 (s), 2954 (w), 2850 (w), 2718 (w), 2360 (w), 2342 (w), 1604 (s), 1477 (s), 1459 (w), 1394 (m), 1324 (w), 1257 (m), 1188 (w), 1161 (w), 1081 (w), 1059 (w), 1041 (w), 975 (w), 863 (w), 786 (w), 759 (w), 752 (w), 726 (s), 625 (w), 570 (w), 545 (w), 472 (w), 400 cm<sup>-1</sup> (w); MS (Cl); *m/z* (%): 332 (6), 331 (27), 304 (20), 303 (100) [M+H]<sup>+</sup>, 302 (6) [M]<sup>+</sup>; elemental analysis calcd (%) for C<sub>20</sub>H<sub>14</sub>O<sub>3</sub>: C 79.46, H 4.67; found: C 79.60, H 4.79.

**Compound 7b:** Analogous to the synthesis of **7a**, after workup, compound **9b** (250 mg, 0.58 mmol) gave **7b** (170 mg, 0.56 mmol, 96%) as a white solid. M.p. > 410 °C (dec at 370 °C); <sup>1</sup>H NMR (400 MHz, [D<sub>6</sub>]DMSO):  $\delta$  = 9.42 (s, 3H; OH), 6.86–6.84 (m, 3H; Ar-4,5,13-H), 6.77–6.73 (m, 3H; Ar-3,6,14-H), 6.49–6.47 (m, 3H; Ar-2,7,15-H), 6.11 (s, 1H; bridgehead-9-H), 5.71 ppm (s, 1H; bridgehead-10-H); <sup>13</sup>C NMR (100 MHz, [D<sub>6</sub>]DMSO):  $\delta$  = 151.9 (Ar-C-16), 151.8 (Ar-C-1,8), 147.9 (Ar-C-4a,10a), 147.6 (Ar-C-12), 131.5 (Ar-C-11), 131.3 (Ar-C-8a,9a), 125.3 (Ar-C-14), 125.2 (Ar-C-3,6), 114.9 (Ar-C-4,5,13), 112.6 (Ar-C-2,7,15) 46.7 ppm (bridgehead-C-10); IR (KBr pellet):  $\tilde{\nu}$  = 3291 (s), 2990 (w), 2975 (w), 2840 (w), 2706 (w), 1890 (w), 1616 (w), 1591 (m), 1463 (s), 1374 (m), 1316 (m), 1254 (s), 1223 (m), 1182 (w), 1191 (w), 1159 (w), 1075 (w), 1034 (m), 975 (w), 946 (w), 852 (w), 786 (w), 771 (w), 726 (s), 714 (w), 674 (w), 599 (w), 583 (w), 561 (w), 537 (w), 476 (w), 392 cm<sup>-1</sup> (w); MS (Cl); *m/z* (%): 331 (16), 304 (20), 303 (100) [M+H]<sup>+</sup>, 302 (73) [M]<sup>+</sup>, 285 (9); elemental analysis calcd (%) for C<sub>20</sub>H<sub>14</sub>O<sub>3</sub>: C 79.46, H 4.67; found: C 79.61, H 4.76.

**Compound 1:** A suspension of **7a** (290 mg, 0.96 mmol) and HMTA (525 mg, 3.74 mmol, 3.9 equiv) in TFA (6 mL) was stirred at 70 °C under an argon atmosphere. After 16 h, the bright-yellow solution was poured into a mixture of CH<sub>2</sub>Cl<sub>2</sub>/hydrochloric acid (2 M, 1:1 v/v; 200 mL) and stirred overnight at room temperature. After separation of the layers, the aqueous layer was extracted with CH<sub>2</sub>Cl<sub>2</sub> (4 × 200 mL) and the combined organic layer was washed with brine (250 mL). After drying over sodium sulfate and evaporation of the solvent, the residual off-white solid was separated by column chromatography (SiO<sub>2</sub>, CH<sub>2</sub>Cl<sub>2</sub>/ethyl acetate, 10:1 (*R*<sub>f</sub> = 0.76)) to give crude **1**, which was washed with *n*-pentane (40 mL) to give pure **1** (179 mg, 0.46 mmol, 47%) as a white solid. M.p.

300 °C (dec); <sup>1</sup>H NMR (500 MHz, [D<sub>6</sub>]DMSO):  $\delta$  = 11.00 (s, 3H; OH), 9.96 (s, 3H; CHO), 7.53 (d, *J* = 7.6 Hz, 3H; Ar-3,6,15-H), 7.29 (d, 6H; *J* = 7.6 Hz, Ar-4,5,16-H), 6.84 (s, 1H; bridgehead-9-H), 6.02 ppm (s, 1H; bridgehead-10-H); <sup>13</sup>C NMR (125 MHz, [D<sub>6</sub>]DMSO):  $\delta$  = 196.2 (CHO), 154.3 (Ar-C-1,8,13), 153.6 (Ar-C-4a,10a,11), 131.9 (Ar-C-8a,9a,12), 131.4 (Ar-C-3,6,15), 120.0 (Ar-C-2,7,14), 116.8 (Ar-C-4,5,16), 54.4 (bridgehead-C-10), 31.7 ppm (bridgehead-C-9); IR (KBr pellet):  $\tilde{\nu}$  = 3429 (br, w), 2849 (w), 2753 (w), 1660 (s), 1623 (s), 1583 (w), 1494 (m), 1438 (m), 1387 (w), 1355 (w), 1323 (m), 1274 (m), 1232 (m), 1145 (w), 1080 (w), 1036 (w), 1075 (w), 925 (w), 860 (w), 772 (m), 762 (m), 619 (w), 578 (w), 514 (w), 489 (w), 464 cm<sup>-1</sup> (w); MS (Cl); *m/z* (%): 415 (13), 388 (23), 387 (100) [M+H]<sup>+</sup>, 386 (29) [M]<sup>+</sup>; elemental analysis calcd (%) for C<sub>23</sub>H<sub>14</sub>O<sub>6</sub>: C 71.50, H 3.65; found: C 71.76, H 3.81.

**Compound 12:** Compound **1** (100 mg, 0.26 mmol), **11** (83 mg, 0.78 mmol) and 4 Å molecular sieves (3 g) were suspended in dry CH<sub>2</sub>Cl<sub>2</sub> (12 mL) in a screw-capped vial and heated at reflux for 5 h. The resulting yellow solution was filtered through a syringe filter (0.45 µm) and the solvent was removed on a rotary evaporator. After drying in high vacuum (5.4 × 10<sup>-1</sup> mbar, 200 °C, 3 h) **13** was obtained as a yellow solid (124 mg, 0.19 mmol, 73%). M.p. 226 °C; <sup>1</sup>H NMR (300 MHz, [D<sub>6</sub>]DMSO):  $\delta$  = 13.83 (s, 3H; OH), 8.93 (s, 3H; imine-H), 7.35–7.33 (m, 9H; Ar-3,6,15-H, tolyl-3,5-H), 7.27–7.24 (d, *J* = 8.3 Hz, 6H; tolyl-2,6-H), 7.19–7.17 (d, *J* = 7.6 Hz, 3H; Ar-4,5,16-H), 6.92 (s, 1H; bridgehead-9-H), 5.82 (s, 1H; bridgehead-10-H), 2.32 ppm (s, 9H; OCH<sub>3</sub>); <sup>13</sup>C NMR (125 MHz, [D<sub>6</sub>]DMSO):  $\delta$  = 162.7 (imine-C), 154.8 (Ar-C-1,8,13), 150.8 (Ar-C-4a,10,11), 144.9 (tolyl-C-1), 136.6 (tolyl-C-1), 131.3 (Ar-C-8a,9a,12), 130.5 (tolyl-C-3), 130.0 (tolyl-C-2), 121.2 (Ar-C-3,6,15), 117.5 (Ar-C-2,7,14), 115.5 (Ar-C-4,5,16), 54.3 (bridgehead-C-10), 32.0 (bridgehead-C-9), 20.7 ppm (OCH<sub>3</sub>); IR (ATR):  $\tilde{\nu}$  = 3740 (w), 3026 (w), 2920 (w), 2711 (w), 1738 (w), 1618 (s), 1596 (s), 1566 (m), 1508 (m), 1441 (m), 1396 (w), 1368 (w), 1327 (w), 1308 (w), 1278 (m), 1202 (m), 1188 (m), 1188 (m), 1172 (m), 1145 (w), 1110 (w), 1084 (w), 1040 (m), 1017 (w), 973 (w), 943 (w), 875 (m), 819 (s), 786 (m), 758 (m), 722 (w), 710 (w), 669 (w), 643 cm<sup>-1</sup> (w); MS (ESI); *m/z*: 653; elemental analysis calcd (%) for C<sub>44</sub>H<sub>35</sub>N<sub>3</sub>O<sub>3</sub>: C 80.83, H 5.40, N 6.33.

**Compound 3:** Compounds **1** (60 mg, 116 µmol) and **2** (46.4 mg, 116 µmol) were dissolved in dry DMF (24 mL) and a solution of TFA in DMF (0.1 M, 32 µL) was added. The mixture was stirred under argon in a screw-capped vial at 120 °C for 3 days. The resulting yellow suspension was allowed to settle at room temperature and the supernatant solution was removed with a Pasteur pipette. The residual suspension was immersed in dry diethyl ether (15 mL). Solvent was removed after 24 h and the process was repeated three times. Finally, the suspension was filtered and the obtained yellow solid was washed three times with dry diethyl ether (10 mL) to give, after drying in vacuo, compound **3** as a yellow solid (48 mg, 19 µmol, 65%). M.p. > 310 °C; <sup>13</sup>C CP MAS NMR:  $\delta$  = 156.6, 145.5, 132.7, 123.5, 117.8, 114.0, 112.6, 110.6, 55.3, 55.0, 32.6 ppm; IR (ATR):  $\tilde{\nu}$  = 2957 (w), 1706 (w), 1615 (s), 1596 (s), 1466 (m), 1439 (m), 1361 (w), 1325 (w), 1276 (w), 1220 (m), 1143 (w), 1082 (w), 1039 (w), 950 (w), 847 (w), 808 (w), 773 (w), 762 (w), 626 cm<sup>-1</sup> (w); MS (MALDI-TOF): *m/z*: 2525.3; elemental analysis calcd (%) for C<sub>172</sub>H<sub>100</sub>N<sub>12</sub>O<sub>12</sub>·17H<sub>2</sub>O: C 72.92, H 4.77, N 5.93; found: C 72.99, H 4.49, N 5.94.

## Acknowledgements

We would like to thank the "Fonds der Chemischen Industrie" (FCI) and the "Deutsche Forschungsgemeinschaft" (DFG) for financial support (project MA4061/4-2) and ChemPur as well as

Solvay Fluor for the donation of chemicals. S.M.E. would like to thank the Studienstiftung des Deutschen Volkes for a scholarship. We also would like to thank Petra Krämer for IR, Bernd Kohl for TGA, Dr. Gang Zhang for gas sorption and Hendrik Herrmann (all University of Heidelberg) for PXRD measurements.

**Keywords:** cage compounds · carbon dioxide capture · cycloaddition · microporous materials · Schiff bases

- [1] D. J. Cram, *Angew. Chem. Int. Ed. Engl.* **1988**, *27*, 1009–1020; *Angew. Chem.* **1988**, *100*, 1041–1052.
- [2] a) G. Zhang, M. Mastalerz, *Chem. Soc. Rev.* **2014**, *43*, 1934–1947; b) C. Seel, F. Vögtle, *Angew. Chem. Int. Ed. Engl.* **1992**, *31*, 528–549; *Angew. Chem.* **1992**, *104*, 542–563.
- [3] W. Kiggen, F. Vögtle, *Angew. Chem. Int. Ed. Engl.* **1984**, *23*, 714–715; *Angew. Chem.* **1984**, *96*, 712–713.
- [4] a) J.-M. Lehn, *Chem. Eur. J.* **1999**, *5*, 2455–2463; b) J.-M. Lehn, *Chem. Soc. Rev.* **2007**, *36*, 151–160; c) P.T. Corbett, J. Leclaire, L. Vial, K. R. West, J.-L. Wietor, J. K. M. Sanders, S. Otto, *Chem. Rev.* **2006**, *106*, 3652–3711.
- [5] M. Mastalerz, *Angew. Chem. Int. Ed.* **2010**, *49*, 5042–5053; *Angew. Chem.* **2010**, *122*, 5164–5175.
- [6] M. L. C. Quan, D. J. Cram, *J. Am. Chem. Soc.* **1991**, *113*, 2754–2755.
- [7] For selected recent examples, see: a) X. Liu, Y. Liu, G. Li, R. Warmuth, *Angew. Chem. Int. Ed.* **2006**, *45*, 901–904; *Angew. Chem.* **2006**, *118*, 915–918; b) X. Liu, R. Warmuth, *J. Am. Chem. Soc.* **2006**, *128*, 14120–14127; c) Y. Liu, X. Liu, R. Warmuth, *Chem. Eur. J.* **2007**, *13*, 8953–8959; d) P. Skowronek, J. Gawronski, *Org. Lett.* **2008**, *10*, 4755–4758; e) O. Francesconi, A. Ienco, G. Moneti, C. Nativi, S. Roelens, *Angew. Chem. Int. Ed.* **2006**, *45*, 6693–6696; *Angew. Chem.* **2006**, *118*, 6845–6848; f) M. Arunachalam, I. Ravikumar, P. Ghosh, *J. Org. Chem.* **2008**, *73*, 9144–9147; g) P. Mateus, R. Delgado, P. Brando, V. Felix, *J. Org. Chem.* **2009**, *74*, 8638–8646; h) X.-N. Xu, L. Wang, G.-T. Wang, J.-B. Lin, G.-Y. Li, X.-K. Jiang, Z.-T. Li, *Chem. Eur. J.* **2009**, *15*, 5763–5774; i) N. Christinat, R. Scopelliti, K. Severin, *Angew. Chem. Int. Ed.* **2008**, *47*, 1848–1852; *Angew. Chem.* **2008**, *120*, 1874–1878; j) B. Icli, N. Christinat, J. Tönnemann, C. Schüttler, R. Scopelliti, K. Severin, *J. Am. Chem. Soc.* **2009**, *131*, 3154–3155; k) A. Granzhan, T. Riis-Johannessen, R. Scopelliti, K. Severin, *Angew. Chem. Int. Ed.* **2010**, *49*, 5515–5518; *Angew. Chem.* **2010**, *122*, 5647–5650; l) A. Granzhan, C. Schouwley, T. Riis-Johannessen, R. Scopelliti, K. Severin, *J. Am. Chem. Soc.* **2011**, *133*, 7106–7115; m) M. Hutin, G. Bernardinelli, J. R. Nitschke, *Chem. Eur. J.* **2008**, *14*, 4585–4593; n) Z. Lin, T. J. Emge, R. Warmuth, *Chem. Eur. J.* **2011**, *17*, 9395–9405; o) J. Sun, R. Warmuth, *Chem. Commun.* **2011**, *47*, 9351–9353; p) Z. Lin, J. Sun, B. Efremovska, R. Warmuth, *Chem. Eur. J.* **2012**, *18*, 12864–12872; q) K. E. Jelfs, X. Wu, M. Schmidtmann, J. T. A. Jones, J. E. Warren, D. J. Adams, A. I. Cooper, *Angew. Chem. Int. Ed.* **2011**, *50*, 10653–10656; *Angew. Chem.* **2011**, *123*, 10841–10844; r) K. Acharyya, P. S. Mukherjee, *Chem. Eur. J.* **2014**, *20*, 1646–1657; s) K. Acharyya, S. Mukherjee, P. S. Mukherjee, *J. Am. Chem. Soc.* **2013**, *135*, 554–557; t) Y. Jin, B. A. Voss, A. Jin, H. Long, R. D. Noble, W. Zhang, *J. Am. Chem. Soc.* **2011**, *133*, 6650–6658; u) Y. Jin, B. A. Voss, R. D. Noble, W. Zhang, *Angew. Chem. Int. Ed.* **2010**, *49*, 6348–6351; *Angew. Chem.* **2010**, *122*, 6492–6495; v) K. D. Okochi, G. S. Han, I. M. Aldridge, Y. Liu, W. Zhang, *Org. Lett.* **2013**, *15*, 4296–4299; w) Y. Jin, A. Athena, R. McCaffrey, H. Long, W. Zhang, *J. Org. Chem.* **2012**, *77*, 7392–7400; x) M. Mastalerz, *Chem. Commun.* **2008**, 4756–4758; y) P. Skowronek, B. Warzajtis, U. Rychlewska, J. Gawronski, *Chem. Commun.* **2013**, *49*, 2524–2526.
- [8] T. Tozawa, J. T. A. Jones, S. I. Swamy, S. Jiang, D. J. Adams, S. Shakespeare, R. Clowes, D. Bradshaw, T. Hasell, S. Y. Chong, C. Tang, S. Thompson, J. Parker, A. Trewin, J. Basca, A. M. Z. Slawin, A. Steiner, A. I. Cooper, *Nat. Mater.* **2009**, *8*, 973–978.
- [9] J. Tian, P. K. Thallapally, S. J. Dalgarno, P. B. McGrail, J. L. Atwood, *Angew. Chem. Int. Ed.* **2009**, *48*, 5492–5495; *Angew. Chem.* **2009**, *121*, 5600–5603.
- [10] For reviews on porous molecular materials, see: a) M. Mastalerz, *Synlett* **2013**, *24*, 781–786; b) J. Tian, P. K. Thallapally, B. P. McGrail, *CrystEngComm* **2012**, *14*, 1909–1919; c) N. B. McKeown, *J. Mater. Chem.* **2010**, *20*, 10588–10597; d) J. R. Holst, A. Trewin, A. I. Cooper, *Nat. Chem.* **2010**, *2*, 915–920.
- [11] For a concept paper on the construction of porous molecular materials, see: M. Mastalerz, *Chem. Eur. J.* **2012**, *18*, 10082–10091.
- [12] a) M. Mastalerz, M. W. Schneider, I. M. Oppel, O. Presly, *Angew. Chem. Int. Ed.* **2011**, *50*, 1046–1051; *Angew. Chem.* **2011**, *123*, 1078–1083; b) M. W. Schneider, H.-J. S. Hauswald, R. Stoll, M. Mastalerz, *Chem. Commun.* **2012**, *48*, 9861–9863; c) M. W. Schneider, I. M. Oppel, M. Mastalerz, *Chem. Eur. J.* **2012**, *18*, 4156–4160; d) M. W. Schneider, I. M. Oppel, H. Ott, L. G. Lechner, H.-J. S. Hauswald, R. Stoll, M. Mastalerz, *Chem. Eur. J.* **2012**, *18*, 836–847; e) M. W. Schneider, L. G. Lechner, M. Mastalerz, *J. Mater. Chem.* **2012**, *22*, 7113–7116; f) G. Zhang, O. Presly, F. White, I. M. Oppel, M. Mastalerz, *Angew. Chem. Int. Ed.* **2014**, *53*, 1516–1520; *Angew. Chem.* **2014**, *126*, 1542–1546; g) G. Zhang, O. Presly, F. White, I. M. Oppel, M. Mastalerz, *Angew. Chem. Int. Ed.* **2014**, *53*, 5126–5130; *Angew. Chem.* **2014**, *126*, 5226–5230.
- [13] a) T. Hasell, M. Schmidtmann, A. I. Cooper, *J. Am. Chem. Soc.* **2011**, *133*, 14920–14923; b) J. T. A. Jones, D. Holden, T. Mitra, T. Hassel, D. J. Adams, K. E. Jelfs, A. Trewin, D. J. Willock, G. M. Day, J. Bacsa, A. Steiner, A. I. Cooper, *Angew. Chem. Int. Ed.* **2011**, *50*, 749–753; *Angew. Chem.* **2011**, *123*, 775–779; c) S. Jiang, J. Bacsa, X. Wu, J. T. A. Jones, R. Dawson, A. Trewin, D. J. Adams, A. I. Cooper, *Chem. Commun.* **2011**, *47*, 8919–8921; d) M. J. Bojdys, M. E. Briggs, J. T. A. Jones, D. J. Adams, S. Y. Chong, M. Schmidtmann, A. I. Cooper, *J. Am. Chem. Soc.* **2011**, *133*, 16566–16571; e) T. Mitra, X. Wu, R. Clowes, J. T. A. Jones, K. Jelfs, D. J. Adams, A. Trewin, J. Bacsa, A. Steiner, A. I. Cooper, *Chem. Eur. J.* **2011**, *17*, 10235–10240; f) J. T. A. Jones, T. Hasell, X. Wu, J. Bacsa, K. E. Jelfs, M. Schmidtmann, S. Y. Chong, D. J. Adams, A. Trewin, F. Schiffman, F. Cora, B. Slater, A. Steiner, G. M. Day, A. I. Cooper, *Nature* **2011**, *474*, 367–371; g) T. Hasell, S. Y. Chong, K. E. Jelfs, D. J. Adams, A. I. Cooper, *J. Am. Chem. Soc.* **2012**, *134*, 588–598; h) M. J. Bojdys, T. Hasell, N. Severin, K. E. Jelfs, J. P. Rabe, A. I. Cooper, *Chem. Commun.* **2012**, *48*, 11948–11950; i) A. Avellaneda, P. Valente, A. Burgun, J. D. Evans, A. W. Markwell-Heys, D. Rankine, D. J. Nielsen, M. R. Hill, C. J. Sumby, C. J. Doonan, *Angew. Chem. Int. Ed.* **2013**, *52*, 3746–3746; *Angew. Chem.* **2013**, *125*, 3834–3837; j) J. D. Evans, D. M. Huang, M. R. Hill, C. J. Sumby, A. W. Thornton, C. J. Doonan, *J. Phys. Chem. C* **2014**, *118*, 1523–1529; k) M. A. Little, S. Y. Chong, M. Schmidtmann, T. Hasell, A. I. Cooper, *Chem. Commun.* **2014**, *50*, 9465–9468; l) T. Hasell, J. L. Culshaw, S. Y. Chong, M. Schmidtmann, M. A. Little, K. E. Jelfs, E. O. Pyzer-Knapp, H. Shepherd, D. J. Adams, G. M. Day, A. I. Cooper, *J. Am. Chem. Soc.* **2014**, *136*, 1438–1448; m) L. Chen, P. S. Reiss, S. Y. Chong, D. Holden, K. E. Jelfs, T. Hasell, M. A. Little, A. Kewley, M. E. Briggs, A. Stephenson, K. M. Thomas, J. A. Armstrong, J. Bell, J. Busto, R. Noel, J. Liu, D. M. Strachan, P. K. Thallapally, A. I. Cooper, *Nat. Mater.* **2014**, *13*, 954–960.
- [14] a) O. K. Farha, I. Eryazici, N. C. Jeong, B. G. Hauser, C. E. Wilmer, A. A. Sarjeant, R. Q. Snurr, S. T. Nguyen, A. O. Yazaydin, J. T. Hupp, *J. Am. Chem. Soc.* **2012**, *134*, 15016–15021; b) H. Furukawa, N. Ko, Y. B. Go, N. Aratani, S. B. Choi, E. Choi, A. Ö. Yazaydin, R. Q. Snurr, M. O'Keeffe, J. Kim, O. M. Yaghi, *Science* **2010**, *329*, 424–428; c) O. K. Farha, A. Ö. Yazaydin, I. Eryazici, C. D. Malliakas, B. G. Hauser, M. G. Kanatzidis, S. T. Nguyen, R. Q. Snurr, J. T. Hupp, *Nat. Chem.* **2010**, *2*, 944–948; d) G. Férey, C. Mellot-Draznieks, C. Serre, F. Millange, J. Dutour, S. Surblé, I. Margiolaki, *Science* **2005**, *309*, 2040–2042.
- [15] T. Hasell, H. Zhang, A. I. Cooper, *Adv. Mater.* **2012**, *24*, 5732–5737.
- [16] A. F. Bushell, P. M. Budd, M. P. Attfield, J. T. A. Jones, T. Hasell, A. I. Cooper, P. Bernardo, F. Bazzarelli, G. Clarizia, J. C. Jansen, *Angew. Chem.* **2013**, *125*, 1291–1294; *Angew. Chem. Int. Ed.* **2013**, *52*, 1253–1256.
- [17] T. Hasell, S. Y. Chong, M. Schmidtmann, D. J. Adams, A. I. Cooper, *Angew. Chem.* **2012**, *124*, 7266–7269; *Angew. Chem. Int. Ed.* **2012**, *51*, 7154–7157.
- [18] a) M. Brutschy, M. W. Schneider, M. Mastalerz, S. R. Waldvogel, *Adv. Mater.* **2012**, *24*, 6049–6052; b) M. Brutschy, M. W. Schneider, M. Mastalerz, S. R. Waldvogel, *Chem. Commun.* **2013**, *49*, 8398–8400.
- [19] M. Liu, A. Little, K. E. Jelfs, J. T. A. Jones, M. Schmidtmann, S. Y. Chong, T. Hasell, A. I. Cooper, *J. Am. Chem. Soc.* **2014**, *136*, 7583–7586.
- [20] M. W. Schneider, I. M. Oppel, A. Griffin, M. Mastalerz, *Angew. Chem. Int. Ed.* **2013**, *52*, 3611–3615; *Angew. Chem.* **2013**, *125*, 3699–3704.
- [21] a) D. Xu, R. Warmuth, *J. Am. Chem. Soc.* **2008**, *130*, 7520–7521; b) M. E. Briggs, K. E. Jelfs, S. Y. Chong, C. Lester, M. Schmidtmann, D. J. Adams,

- A. I. Cooper, *Cryst. Growth Des.* **2013**, *13*, 4993–5000; c) S. Klotzbach, T. Scherpel, F. Beuerle, *Chem. Commun.* **2014**, *50*, 12454–12457.
- [22] C. Zhang, C. Chen, *J. Org. Chem.* **2006**, *71*, 6626–6629.
- [23] a) L. J. Abbott, A. G. McDermott, A. Del Rego, R. G. D. Taylor, C. G. Bezzu, K. J. Msayib, N. B. McKeown, F. R. Siperstein, J. Runt, C. M. Colina, *J. Phys. Chem. B* **2013**, *117*, 355–364; b) A. Del Rego, F. R. Siperstein, R. G. D. Taylor, N. B. McKeown, *Microporous Mesoporous Mater.* **2013**, *176*, 55–63; c) L. J. Abbott, N. B. McKeown, C. M. Colina, *J. Mater. Chem. A* **2013**, *1*, 11950–11960.
- [24] a) P. D. Bartlett, M. J. Ryan, S. G. Cohen, *J. Am. Chem. Soc.* **1942**, *64*, 2649–2653; b) G. Wittig, E. Benz, *Angew. Chem.* **1958**, *70*, 166.
- [25] J. H. Chong, M. J. MacLachlan, *Inorg. Chem.* **2006**, *45*, 1442–1444.
- [26] P.-F. Li, C.-F. Chen, *J. Org. Chem.* **2012**, *77*, 9250–9259.
- [27] a) H. Tanida, R. Muneyuki, *J. Am. Chem. Soc.* **1965**, *87*, 4794–4804; b) M. W. Galley, R. C. Hahn, *J. Org. Chem.* **1976**, *41*, 2006–2009.
- [28] I. Mori, T. Kadosaka, Y. Sakata, S. Misumi, *Bull. Chem. Soc. Jpn.* **1971**, *44*, 1649–1652.
- [29] M. Rogers, B. Averill, *J. Org. Chem.* **1986**, *51*, 3308–3314.
- [30] D. Pena, A. Cobas, D. Perez, E. Guitián, *Synthesis* **2002**, *10*, 1454–1458.
- [31] Y. Li, R. Cao, S. J. Lippard, *Org. Lett.* **2011**, *13*, 5052–5055.
- [32] J. Chmiel, I. Heesemann, A. Mix, B. Neumann, H.-G. Stammmer, N. W. Mitzel, *Eur. J. Org. Chem.* **2010**, 3897–3907.
- [33] a) R. Huisgen, J. Sauer, *Angew. Chem.* **1960**, *72*, 91–108; b) H. Heaney, *Chem. Rev.* **1962**, *62*, 81–97; c) R. Hoffmann, A. Imamura, W. J. Hehre, *J. Am. Chem. Soc.* **1968**, *90*, 1499–1509.
- [34] CCDC 1017925 (**rac-6c**), 1017926 (**rac-6d**), 1017927 (**8a**), 1017928 (**9a**), 1017929 (**9b**), 1017930 (**10a**), 1017931 (**11**) and 1017932 (**13**) contain the supplementary crystallographic data for this paper. These data can be obtained free of charge from The Cambridge Crystallographic Data Centre via [www.ccdc.cam.ac.uk/data\\_request/cif](http://www.ccdc.cam.ac.uk/data_request/cif).
- [35] B. Klanderman, *J. Am. Chem. Soc.* **1965**, *87*, 4649–4651.
- [36] R. G. D. Taylor, M. Carta, C. G. Bezzu, J. Walker, K. J. Msayib, B. M. Kariuki, N. B. McKeown, *Org. Lett.* **2014**, *16*, 1848–1851.
- [37] C. E. Godinez, G. Zepeda, C. J. Mortko, H. Dang, M. A. Garcia-Garibay, *J. Org. Chem.* **2004**, *69*, 1652–1662.
- [38] J. Rigaudy, M. Ricard, *Tetrahedron* **1968**, *24*, 3241–3245.
- [39] a) M. Kloetzel, R. Dayton, H. Herzog, *J. Am. Chem. Soc.* **1950**, *72*, 273–277; b) M. Kloetzel, H. Herzog, *J. Am. Chem. Soc.* **1950**, *72*, 1991–1995; c) W. Jones, D. Mangold, H. Plieninger, *Tetrahedron* **1962**, *18*, 267–272; d) F. Klärner, V. Breitkopf, *Eur. J. Org. Chem.* **1999**, 2757–2762; e) G. G. Iskhakova, V. D. Kiselev, E. A. Kashaeva, L. N. Potapova, E. A. Berdnikov, D. B. Krivolapov, I. A. Litvinov, *ARKIVOC* **2004**, *12*, 70–79; f) Y. He, C. Junk, D. Lemal, *Org. Lett.* **2003**, *5*, 2135–2136; g) T. Murase, S. Horiuchi, M. Fujita, *J. Am. Chem. Soc.* **2010**, *132*, 2866–2867.
- [40] In UPLC-MS analysis of the combined washing solution from which **rac-6c** and **rac-6d** have been isolated, only two signals were obtained with *m/z* 344 (**rac-6c**) and 450 (**rac-6d**) when various columns and eluent mixtures were applied. Also, by <sup>1</sup>H NMR spectroscopy, no indication was found for the potential formation of other stereo- or regioisomers.
- [41] J. Duff, E. Bills, *J. Chem. Soc.* **1934**, *2*, 1305–1308.
- [42] A. K. Unni, N. Takenaka, H. Yamamoto, V. H. Rawal, *J. Am. Chem. Soc.* **2005**, *127*, 1336–1337.
- [43] M. Perrin, C. Bavourx, A. Thozet, *Acta Cryst. Sect. B* **1977**, *33*, 3516–3520.
- [44] G. Gilli, F. Bellucci, V. Ferretti, V. Bertolas, *J. Am. Chem. Soc.* **1989**, *111*, 1023–1028.
- [45] a) CrystalExplorer (Version 3.1): S. K. Wolff, D. J. Grimwood, J. J. McKinnon, M. J. Turner, D. Jayatilaka, M. A. Spackman, University of Western Australia, **2012**; b) M. J. Turner, J. J. McKinnon, D. Jayatilaka, M. A. Spackman, *CrystEngComm* **2011**, *13*, 1804–1813.
- [46] a) K. Ogawa, Y. Kasahara, Y. Ohtani, J. Harada, *J. Am. Chem. Soc.* **1998**, *120*, 7107–7108; b) J. Harada, H. Uekusa, Y. Ohashi, *J. Am. Chem. Soc.* **1999**, *121*, 5809–5810.
- [47] R. Subramanian, S. A. Koch, G. S. Harbison, *J. Phys. Chem.* **1993**, *97*, 8625–8629.
- [48] T. Hasell, M. Schmidtmann, C. A. Stone, M. W. Smith, A. I. Cooper, *Chem. Commun.* **2012**, *48*, 4689–4691.
- [49] T. Hasell, X. Wu, J. T. A. Jones, J. Bacsa, A. Steiner, T. Mitra, A. Trewin, D. J. Adams, A. I. Cooper, *Nat. Chem.* **2010**, *2*, 750–755.
- [50] K. Sing, D. H. Everett, R. A. W. Haul, L. Moscou, R. A. Pierotti, J. Rouquerol, T. Siemieniewska, *Pure Appl. Chem.* **1985**, *57*, 603–619.
- [51] B. C. Lippens, J. H. de Boer, *J. Catal.* **1965**, *4*, 319–323.
- [52] G. Y. Gor, M. Thommes, K. A. Cybosz, A. V. Neimark, *Carbon* **2012**, *50*, 1583–1590.
- [53] S. Jiang, K. E. Jelfs, D. Holden, T. Hasell, S. Y. Chong, M. Haranczyk, A. Trewin, A. I. Cooper, *J. Am. Chem. Soc.* **2013**, *135*, 17818–17830.
- [54] a) J. H. Chong, S. J. Ardakani, K. J. Smith, M. J. MacLachlan, *Chem. Eur. J.* **2009**, *15*, 11824–11828; b) J. Tian, P. Thallapally, J. Liu, G. J. Exharhos, J. L. Atwood, *Chem. Commun.* **2011**, *47*, 701–703; c) B. Kohl, F. Rominger, M. Mastalerz, *Org. Lett.* **2014**, *16*, 704–707.
- [55] M. Mastalerz, I. M. Oppel, *Angew. Chem. Int. Ed.* **2012**, *51*, 5252–5255; *Angew. Chem.* **2012**, *124*, 5345–5348.
- [56] a) L. Espinal, D. L. Poster, W. Wong-Ng, A. J. Allen, M. L. Green, *Environ. Sci. Technol.* **2013**, *47*, 11960–11975; b) S. D. Kenarsari, D. Yang, G. Jiang, S. Zhang, J. Wang, A. G. Russell, Q. Wie, M. Fan, *RSC Adv.* **2013**, *3*, 22739–22773; c) K. Sumida, D. L. Rogow, J. A. Mason, T. M. McDonald, E. D. Bloch, Z. R. Herm, T.-H. Bae, J. R. Long, *Chem. Rev.* **2012**, *112*, 724–781; d) J. Liu, P. K. Thallapally, B. P. McGrail, D. R. Brown, J. Liu, *Chem. Soc. Rev.* **2012**, *41*, 2308–2322; e) N. Gargiulo, F. Pepe, D. Caputo, J. Nanosci. Nanotechnol. **2014**, *14*, 1811–1822; f) R. Sabouni, H. Kazemian, S. Rohani, *Environ. Sci. Pollut. Res. Int.* **2014**, *21*, 5427–5449.
- [57] a) J. Tóth, *Adv. Colloid Interface Sci.* **1995**, *55*, 1; b) J. Tóth, *Modelling and Analysis*, Dekker, New York, **2002**; c) W. Yang, A. Greenaway, X. Lin, R. Matsuda, A. J. Blake, C. Wilson, W. Lewis, P. Hubberstey, S. Kitagawa, N. R. Champness, M. Schröder, *J. Am. Chem. Soc.* **2010**, *132*, 14457–14469; d) E. Neofotistou, C. D. Malliakas, P. N. Trikalitis, *Chem. Eur. J.* **2009**, *15*, 4523–4527.
- [58] Z. Bao, L. Yu, Q. Ren, X. Lu, S. Deng, *J. Colloid Interface Sci.* **2011**, *353*, 549–556.
- [59] M. G. Rabbani, H. M. El-Kaderi, *Chem. Mater.* **2012**, *24*, 1511–1517.
- [60] B. Panella, M. Hirscher, H. Pütter, U. Müller, *Adv. Funct. Mater.* **2006**, *16*, 520–524.
- [61] N. T. Nguyen, H. Furukawa, F. Gándara, H. T. Nguyen, K. E. Cordova, O. M. Yaghi, *Angew. Chem. Int. Ed.* **2014**, *53*, 10645–10648; *Angew. Chem.* **2014**, *126*, 10821–10824.
- [62] S. Yang, X. Lin, W. Lewis, M. Suyetin, E. Bichoutskaia, J. E. Parker, C. C. Tang, D. R. Allan, P. J. Rizkallah, P. Hubberstey, N. R. Champness, K. M. Thomas, A. J. Blake, M. Schröder, *Nat. Mater.* **2012**, *11*, 710–716.
- [63] a) M. Mastalerz, S. Sieste, M. Cenic, I. M. Oppel, *J. Org. Chem.* **2011**, *76*, 6389–6393; b) D. Anselmo, G. Salassa, E. C. Escudero-Adán, E. Martin, A. W. Kleij, *Dalton Trans.* **2013**, *42*, 7962–7970; c) S. Akine, S. Piao, M. Miyashita, T. Nabeshima, *Tetrahedron Lett.* **2013**, *54*, 6541–6544; d) S. Akine, M. Miyashita, S. Piao, T. Nabeshima, *Inorg. Chem. Front.* **2014**, *1*, 53–57.
- [64] M. Mastalerz, H.-J. S. Hauswald, R. Stoll, *Chem. Commun.* **2012**, *48*, 130–132.
- [65] G. M. Sheldrick, *Acta Crystallogr. Sect. A* **2008**, *65*, 112–122.
- [66] G. M. Sheldrick, Bruker Analytical X-ray Division, Madison, Wisconsin, USA, **2008**.
- [67] D. Hellwinkel, *Die Systematische Nomenklatur Der Organischen Chemie: Eine Gebrauchsanweisung*, Springer, Heidelberg, **2006**.

Received: August 12, 2014

Published online on October 21, 2014